THE JOURNAL OF BIOLOGICAL CHEMISTRY VOL. 287, NO. 33, pp. 27417–27430, August 10, 2012

γ-Aminobutyric Acid Type A ($GABA_A$) Receptor α Subunits Play a Direct Role in Synaptic *Versus* Extrasynaptic Targeting*[S]◆

Received for publication, March 9, 2012, and in revised form, May 31, 2012 Published, JBC Papers in Press, June 18, 2012, DOI 10.1074/jbc.M112.360461

Xia Wu[‡], Zheng Wu[‡], Gang Ning[‡], Yao Guo[‡], Rashid Ali[§], Robert L. Macdonald[¶], Angel L. De Blas[§], Bernhard Luscher[‡‖], and Gong Chen[‡1]

From the Departments of [‡]Biology and [‖]Biochemistry and Molecular Biology, Huck Institutes of Life Sciences, Pennsylvania State University, University Park, Pennsylvania 16802, the [§]Department of Physiology and Neurobiology, University of Connecticut, Storrs, Connecticut 06269, and the [¶]Department of Neurology, Vanderbilt University Medical Center, Nashville, Tennessee 37212

Background: $GABA_A$ receptor γ2 and δ subunits are thought to be responsible for synaptic and extrasynaptic targeting.
Results: We demonstrate here that α2 and α6 subunits can target δ/γ2 chimeras to synaptic and extrasynaptic sites.
Conclusion: The α subunits play a direct role in $GABA_A$ receptor targeting.
Significance: Different subunits of $GABA_A$ receptors encode intrinsic signals to control subcellular targeting.

$GABA_A$ receptors ($GABA_A$-Rs) are localized at both synaptic and extrasynaptic sites, mediating phasic and tonic inhibition, respectively. Previous studies suggest an important role of γ2 and δ subunits in synaptic *versus* extrasynaptic targeting of $GABA_A$-Rs. Here, we demonstrate differential function of α2 and α6 subunits in guiding the localization of $GABA_A$-Rs. To study the targeting of specific subtypes of $GABA_A$-Rs, we used a molecularly engineered GABAergic synapse model to precisely control the $GABA_A$-R subunit composition. We found that in neuron-HEK cell heterosynapses, GABAergic events mediated by $\alpha2\beta3\gamma2$ receptors were very fast (rise time ~2 ms), whereas events mediated by $\alpha6\beta3\delta$ receptors were very slow (rise time ~20 ms). Such an order of magnitude difference in rise time could not be attributed to the minute differences in receptor kinetics. Interestingly, synaptic events mediated by $\alpha6\beta3$ or $\alpha6\beta3\gamma2$ receptors were significantly slower than those mediated by $\alpha2\beta3$ or $\alpha2\beta3\gamma2$ receptors, suggesting a differential role of α subunit in receptor targeting. This was confirmed by differential targeting of the same δ-γ2 chimeric subunits to synaptic or extrasynaptic sites, depending on whether it was co-assembled with the α2 or α6 subunit. In addition, insertion of a gephyrin-binding site into the intracellular domain of α6 and δ subunits brought $\alpha6\beta3\delta$ receptors closer to synaptic sites. Therefore, the α subunits, together with the γ2 and δ subunits, play a critical role in governing synaptic *versus* extrasynaptic targeting of $GABA_A$-Rs, possibly through differential interactions with gephyrin.

Neural inhibition in the brain is mostly mediated by $GABA_A$ receptors ($GABA_A$-Rs).[2] To date, 19 isoforms of $GABA_A$-R subunits have been identified as follows: α1–6, β1–3, γ1–3, δ, ϵ, θ, π, and ρ1–3 (1, 2). Most $GABA_A$-Rs expressed in the brain are composed of two α, two β, and one γ subunits, of which the γ subunit can be substituted by δ, ϵ, θ, or π (3, 4).

There are two forms of GABAergic inhibition, phasic and tonic (5, 6). Phasic inhibition is mediated by postsynaptically clustered $GABA_A$-Rs composed of α1–3, β2–3, and γ2 subunits. Tonic inhibition is mediated by extrasynaptic $GABA_A$-Rs typically composed of α4/6 (and possibly α1), β and δ subunits (7–9), as well as $\alpha5\beta\gamma2$ subunits (10–12). Blocking tonic inhibition significantly enhanced neuronal excitability (5, 13–15). Malfunction of tonic inhibition is implicated in epilepsy, abnormal cognition and memory, sleep disorders, anxiety, depression, schizophrenia, and alcohol addiction (16–23).

Although the mechanisms for synaptic receptor targeting have been extensively studied, little is known about the molecular mechanisms specifying extrasynaptic targeting of δ subunit-containing $GABA_A$-Rs. Neurons deficient in the α1 or α2 or α3 subunits showed diminished postsynaptic $GABA_A$-R clusters in different subcellular localizations (24–27). The γ2 subunit, and particularly its intracellular loop (IL) and the fourth transmembrane domain (TM4), plays a critical role in synaptic clustering of $GABA_A$-Rs (28–31). In contrast, the δ subunit-containing $GABA_A$-Rs are mainly localized at extrasynaptic membranes (7, 8). Thus, the γ2 and δ subunits have been thought to be involved in the synaptic *versus* extrasynaptic targeting of $GABA_A$-Rs. However, the mostly extrasynaptic $\alpha5\beta\gamma2$ and punctated $\alpha1\beta\delta$ $GABA_A$-Rs suggest that γ2 and δ subunits cannot be solely responsible for guiding $GABA_A$-R targeting (9, 10, 12).

Here, we employed a molecularly engineered synapse model to investigate the mechanism of δ-$GABA_A$-R targeting. We

* This work was supported, in whole or in part, by National Institutes of Health Grants NS054858 from NINDS, MH083911 from NIMH (to G. C.), NS38752 (to A. L. D.) and NS33300 from NINDS (to R. L. M.), and MH062391 from NIMH (to B. L.).
◆ This article was selected as a Paper of the Week.
[S] This article contains supplemental Fig. 1 and Tables 1.
[1] To whom correspondence should be addressed. Tel.: 814-865-2488; E-mail: gongchen@psu.edu.

[2] The abbreviations used are: $GABA_A$-R, $GABA_A$ receptor; IPSC, inhibitory postsynaptic current; THDOC, 3α,21-dihydroxy-5α-preganan-20-one; THIP, 4,5,6,7-tetrahydroisoxazolo[5,4-c]pyridin-3-ol; GBS, gephyrin-binding site; IL, intracellular loop; TM4, fourth transmembrane domain; ANOVA, analysis of variance; GAD, glutamic acid decarboxylase; sIPSC, spontaneous IPSC.

demonstrated that in neuron-HEK cell synapses, distinct subunit combinations control $GABA_A$-R targeting. Electrophysiological as well as immunoelectron microscopic results indicated that in HEK cells, $\alpha2\beta3\gamma2$ receptors cluster at synaptic sites, whereas $\alpha6\beta3\delta$ receptors mainly localize at extrasynaptic membranes. Interestingly, when paired with the same chimeric δ-$\gamma2$ subunit, different α subunits ($\alpha2$ *versus* $\alpha6$) dictated synaptic *versus* extrasynaptic targeting of the corresponding $GABA_A$-Rs. We also showed that molecularly engineered interaction with gephyrin recruited modified $\alpha6\beta\delta$ receptors to synaptic sites. Thus, $GABA_A$-R targeting is controlled by specific subunit composition and the ability to interact with gephyrin.

EXPERIMENTAL PROCEDURES

Cell Culture and Transfection—Astrocytes were cultured from the cortical tissue of neonatal rat pups (postnatal day 3–5) as described before (32, 33). Briefly, cells dissociated from cortices were plated in 25-cm^2 flasks for up to a week, during which time astrocytes grew to confluence, whereas nonastrocytic cells were removed by rigorous shaking. The flat astroglial cells were then trypsinized and replated on poly-D-lysine (0.1 mM)-coated coverslips to serve as a supporting substrate for co-cultured neurons. Hypothalamic cultures were prepared from Sprague-Dawley rat day 18 embryos (of either sex) as described previously (34). The medial hypothalamus was dissected out, cut into small cubes, and digested in 0.05% trypsin/EDTA solution with 50 units/ml DNase I at 37 °C for 25 min. After digestion, the tissue blocks were dissociated into single neurons by gentle trituration and plated on poly-D-lysine-coated coverslips covered by a monolayer of astrocytes at the density of 4000 – 8000 cells/cm^2. The neuronal culture medium contained 500 ml of minimum Eagle's medium (Invitrogen), 5% fetal bovine serum (HyClone, Logan, UT), 10 ml of B-27 supplement (Invitrogen), 100 mg of $NaHCO_3$, 20 mM D-glucose, 0.5 mM L-glutamine, and 25 units/ml penicillin/streptomycin.

Neurons were transfected with a modified Ca^{2+}-phosphate transfection protocol (35). Immunocytochemistry was performed in neurons 24 – 48 h after transfection.

Human embryonic kidney (HEK) 293T cells were maintained in DMEM supplemented with 10% FBS and 25 units/ml penicillin/streptomycin. HEK 293T cells were also transfected with the Ca^{2+}-phosphate transfection method and co-cultured with hypothalamic neurons as described previously (34). In general, 24 h after transfection, HEK cells were dissociated with 0.05% trypsin/EDTA and plated on top of 1-week-old hypothalamic cultures. The cells were utilized for electrophysiological recordings or immunocytochemistry after 2–3 days of co-culture. Each experiment was repeated in at least three independent batches of cultures.

Plasmid Constructs—The CMV-based expression vectors for the $GABA_A$ receptor $\alpha2$, $\beta3$, and $^{myc}\gamma2$ subunits were described previously (30). The $^{myc}\gamma2$ subunit construct contained the Myc 9E10 epitope between the 4th and 5th amino acid of the mature polypeptide. The cDNAs encoding the rat $GABA_A$-R $\alpha6$ and δ subunits were cloned into the expression vector pCMVneo (36). The $\delta/\gamma2$ chimeras (M1i and M2e) were constructed using the splice overhang extension method (37). The rat chimera $\delta/\gamma2$ILTM4 was generated with a two-step strategy to swap the fragment containing the large intracellular loop (IL), the TM4, and the C terminus of the δ subunit with the corresponding one of $\gamma2$S ($\gamma2$ILTM4). In the first step, cmyc-$\gamma2$S in pCDNA3.1 was used as a template in a PCR to amplify a 447-bp fragment. In the second step, this fragment was combined with methylated full-length cmyc-δ (in pcDNA3.1) as a template, using the Invitrogen GeneTailor™ site-directed mutagenesis system. The $\delta/\gamma2$ILTM4 chimeric subunit was sequenced, and the full-length chimeric open reading frame fragment was amplified by PCR using specific primers containing 5′-NheI and 3′-XhoI sites and inserted into pCDNA 3.1 to exclude possible modifications of pcDNA3.1 during the previous steps, followed by sequencing.

To construct the $\alpha6_{\alpha2IL}$ chimera, the $\alpha6$ subunit coding sequence was amplified by PCR from pCMVneo-$\alpha6$ and inserted into pcDNA3.1$^+$ between BamHI and XbaI sites. The coding sequence of the $\alpha2$ subunit IL (amino acids 307–391 of the mature polypeptide) was amplified from the $\alpha2$ construct and inserted between the two EcoRI sites just outside the coding region of the $\alpha6$ subunit IL (amino acids 306 – 400). For the $\alpha2_{\alpha6IL}$ chimera, the rat $\alpha2$ subunit coding sequence was amplified from the $\alpha2$ construct using HindIII and ApaI restriction site-containing primers and inserted into pcDNA3.1$^+$ between HindIII and ApaI sites. An EcoRI site was engineered just upstream of the IL coding region through synonymous mutagenesis at amino acid 303. The EcoRI and XbaI sites around amino acid 16 and 17 were eliminated in the same way to ensure successful insertion of the $\alpha6$ subunit IL-coding sequence. The coding sequence of the $\alpha6$ subunit IL was amplified and inserted between the engineered EcoRI site and an XbaI site just downstream from the $\alpha2$ subunit IL coding region. For both constructions, the sequences outside the ILs were not changed.

δ_{GBS} and $\alpha6_{GBS}$ chimeras were constructed in pCMVneo by insertion of the 18-amino acid gephyrin-binding site (GBS) of the glycine receptor β subunit (38) into the IL of the δ subunit (after amino acid 341 of the mature polypeptide) and the IL of the $\alpha6$ subunit after amino acid 340. Two DNA fragments, one including coding sequences of the target protein from the N terminus to the insertion site and the other including that from the insertion site to the C terminus, were amplified from pCMVneo-$\alpha6$ and pCMVneo-δ. Both fragments also contained partial and overlapping insertion sequences and were fused into one fragment by PCR. The resulting fragment was inserted back into pCMVneo vector.

The murine HA-tagged NL2A expression vector (pNiceNLG-2, referred to as NL2 in this work) was obtained from Dr. P. Scheiffele (University of Basel) (39). The HA tag was inserted between the signal peptide and the N terminus of the mature protein. The gephyrin-GFP construct encodes human gephyrin with GFP fused to the C terminus of gephyrin (40). The collybistin constructs encode two isoforms of human collybistin: $CB3_{SH3+}$/$hPEM2_{SH3+}$ containing the SH3 domain and $CB3_{SH3-}$/$hPEM2_{SH3-}$ lacking the SH3 domain (41).

Electrophysiology—Whole-cell recordings were performed in voltage clamp mode by using Multiclamp 700A amplifier (Molecular Devices, Palo Alto, CA) as described before (42). Patch pipettes were pulled from borosilicate glass and fire-pol-

ished to a resistance of 3–6 megohms. The recording chamber was continuously perfused with a bath solution containing 128 mM NaCl, 30 mM glucose, 25 mM HEPES, 5 mM KCl, 2 mM $CaCl_2$, and 1 mM $MgCl_2$ (pH 7.3, adjusted with NaOH, ~320 mosM). The pipette solution contained 135 mM KCl, 10 mM HEPES, 2 mM EGTA, 10 mM Tris-phosphocreatine, 4 mM MgATP, 0.5 mM Na_2GTP (pH 7.3, adjusted with KOH, ~300 mosM). Data were acquired using the pCLAMP9 software (Molecular Devices), sampled at 5 kHz, filtered at 1 kHz, and analyzed with Clampfit 9.0 (Molecular Devices). Drugs were applied through a fast drug application system (VC-6; Warner Instruments, Hamden, CT) to assess the pharmacological properties of the reconstituted $GABA_A$-Rs, as indicated by the rapid rise phase of whole-cell GABA and THIP currents in the pharmacological study (Fig. 1). Spontaneous IPSCs were recorded with normal bath perfusion. Spontaneous events were analyzed by MiniAnalysis software (Synaptosoft). The 20–80% rising time and the weighted time constant ($\tau_{weighted} = (\tau 1 \times A1 + \tau 2 \times A2)/(A1 + A2)$) of the IPSCs were analyzed to compare the kinetics of the events. Pooled data were presented as means ± S.E., and *n* represents the number of the cells recorded. One-way ANOVA was employed to analyze multiple groups of data, followed by Bonferroni's pairwise comparison.

Ultrafast GABA application and outside-out patch recording were employed to assess the onset kinetics of $GABA_A$-Rs composed of different subunits. The ultrafast drug application system (ALA Inc., Long Island, NY) consists of solution reservoirs, manual switching valves, a solenoid-driven four-way pinch valve, and two tubes (inner diameter 500 μm) oriented at 50° for rapid solution exchange (43, 44). One tube contains normal bath solution and the other contains 10 mM GABA to maximally activate $GABA_A$-Rs. The solution exchange rate was estimated to be within 1 ms (20–80% rise time), using an open tip electrode to detect the junction potential caused by different salt concentrations (75 mM *versus* 150 mM NaCl). Typically, six pulses of GABA were applied to each patch. The duration of GABA application was sufficient (200–500 ms) to reach the peak current value. Data were sampled at 10 kHz and low pass filtered at 4 kHz (8-pole Bessel filter). Individual traces were aligned and averaged, and the 20–80% rising time was analyzed with MiniAnalysis software.

Drugs—GABA, tetrodotoxin, and 3α,21-dihydroxy-5α-pregnan-20-one (THDOC) were obtained from Sigma. Bicuculline methobromide, 6-cyano-7-nitroquinoxaline-2,3-dione, and THIP hydrochloride were purchased from Tocris (Ellisville, MO). 6-Cyano-7-nitroquinoxaline-2,3-dione and THDOC were initially dissolved as concentrated stock solutions in dimethyl sulfoxide (DMSO) and diluted to appropriate concentrations in the bath solution. The final DMSO concentration was lower than 0.1%. Other drugs were first dissolved in deionized water and freshly diluted to the final concentration in bath solution immediately before the experiments.

Immunocytochemistry and Immunoelectron Microscopy—For immunofluorescent stainings, cells were fixed with 4% paraformaldehyde for 12 min and permeabilized with 0.1% Triton X-100 in the blocking solution (PBS with 3% normal goat serum + 2% normal donkey serum) for 30 min at room temperature. The cells were incubated with the primary antibodies at 4 °C overnight, followed by the secondary antibodies at room temperature for 1 h. All antibodies were diluted with the blocking solution. The δ subunit in α6β3δ-transfected neurons was labeled before permeabilization (Fig. 4*A*), and the rest of the stainings were conducted after permeabilization (Figs. 4*B* and 7, *C* and *G–I*). The following primary antibodies were used: rabbit anti-Myc tag (1:200; Millipore, Billerica, MA); rabbit anti-δ-Nterm antibody (1:500; PhosphoSolutions, Aurora, CO); mouse anti-GAD6 (1:100; Developmental Studies Hybridoma Bank), and mouse anti-gephyrin mAb7a (1:500; Synaptic Systems, Goettingen, Germany). Secondary antibodies were as follows: Alexa Fluor 647 goat anti-mouse; Alexa Fluor 546 goat anti-rabbit, and Alexa Fluor 488 donkey anti-rabbit (1:300, Molecular Probes, Eugene, OR).

For the electron microscopy experiments, HEK cells were co-transfected with the following: 1) NL2, α6, β3, and δ; 2) NL2, α2, β3, and γ2-GFP and co-cultured with hypothalamic neurons for 2 days. The cells were briefly fixed with 4% paraformaldehyde + 0.05% glutaraldehyde (10 min at room temperature followed by 20 min in 4 °C), quenched in 0.15% glycine for 10 min, and incubated in blocking solution (3% normal goat serum plus 2% normal donkey serum in bath solution) for 1 h at 4 °C. Primary antibodies were diluted in blocking solution (rabbit anti-δ-Nterm (1:100); rabbit anti-GFP (1:200, Invitrogen)) and applied to the samples at 4 °C overnight. The cells were then incubated with secondary antibodies (1.4 nM Nanogold goat anti-rabbit (1:50; Nanoprobes, Yaphank, NY)) for 1 h at room temperature, fixed with 1% glutaraldehyde for 20 min, and processed with the HQ silver enhancement kit (Nanoprobes, Yaphank, NY) according to the instructions. After developing with the silver enhancer, the cells were submerged in 2% glutaraldehyde, scraped off from the coverslips, and centrifuged at 8000 relative centrifugal force for 10 min to collect the cells. The pellets were further fixed with 2% glutaraldehyde for 1 h at room temperature before EM processing. The cell pellets were post-fixed in 1% OsO_4 for 1 h. The cells were then dehydrated in a serial of graded ethanol solutions and embedded in Eponite 12. Thin sections (80 nm) were cut with a Leica UC6 ultramicrotome, contracted with uranyl acetate and lead citrate, and examined in a TEM JEOL JEM 1200 EXII (Peabody, MA) at 80 kV. Hetero-synapses were identified by nerve terminals (filled with synaptic vesicles) apposing HEK cells that showed immunogold puncta on the plasma membrane. The edge of synapses was defined as the point where the plasma membrane of nerve terminals starts to diverge from HEK cell membrane. The localization of silver-enhanced gold labeling of $GABA_A$-Rs was characterized into three categories as follows: 1) synaptic, inside a synapse, and more than 30 nm away from the edges; 2) perisynaptic, less than 30 nm away from the synaptic edges; and 3) extrasynaptic, outside synapses, and over 30 nm away from the edges of synapses (8).

Co-immunoprecipitation—HEK cells were transfected with either δ or δ_{GBS} together with gephyrin-GFP. Gephyrin-GFP single transfection served as the control. Rabbit anti-δ-Nterm was used for the immunoprecipitation, and rabbit anti-GFP was used in the immunoblotting to detect the gephyrin-GFP.

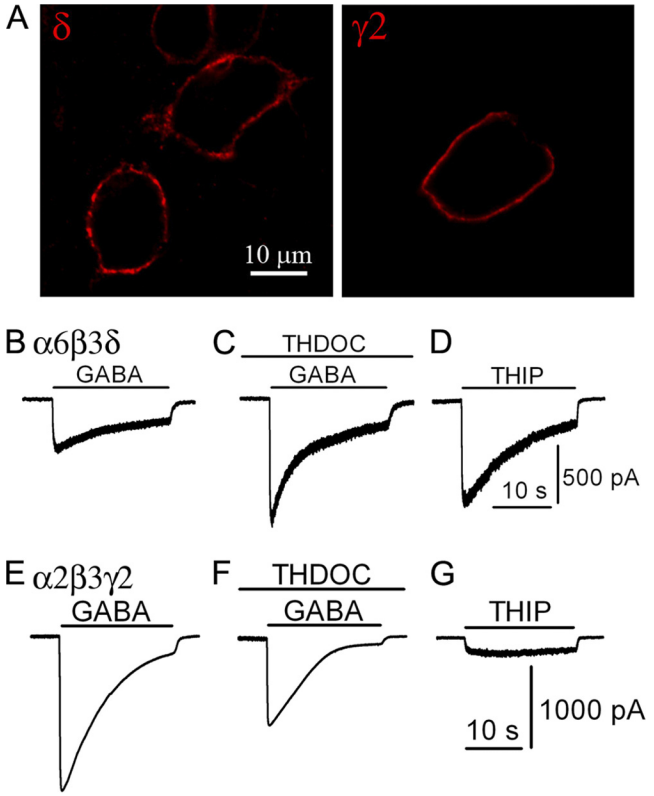

FIGURE 1. **Recombinant GABA$_A$-Rs with distinct pharmacological properties.** *A,* comparable expression level of $\alpha2\beta3\gamma2$ and $\alpha6\beta3\delta$ receptors on HEK cell membranes, revealed by surface staining without permeabilization. *B–D,* pharmacological responses of HEK 293T cells co-expressing $\alpha6$, $\beta3$, and δ subunits. *B,* representative trace showing the whole-cell GABA (100 μM) current in a HEK 293T cell transfected with $\alpha6\beta3\delta$. *C,* positive modulation of GABA-induced current by a neurosteroid THDOC (100 nM). *D,* THIP (100 μM) acts as a super-agonist on $\alpha6\beta3\delta$ GABA$_A$-Rs. *E–G,* pharmacological responses of HEK 293T cells co-expressing $\alpha2$, $\beta3$, and $\gamma2$ subunits. *E,* representative trace showing whole-cell GABA (100 μM) current in a $\alpha2\beta3\gamma2$-transfected HEK 293T cells. *F,* GABA induces a smaller whole-cell current in the presence of THDOC (100 nM). *G,* THIP acts as a partial agonist for the $\alpha2\beta3\gamma2$-GABA$_A$-Rs.

RESULTS

Distinct Pharmacological Properties of Heterologously Expressed GABA$_A$-Rs—Neurons express a broad spectrum of GABA$_A$-Rs composed of different subunits, making it difficult to identify the critical factors important for the targeting of a specific receptor subtype. We therefore employed our recently established hetero-synapse system to investigate the targeting of different subtypes of GABA$_A$-Rs (34). When HEK cells were transfected with GABA$_A$-R subunits and a cell adhesion molecule neuroligin-2 (NL2) and then co-cultured with neurons, both spontaneous and action potential-evoked GABAergic events were detected (34). With this system, we can precisely control the subunit composition of GABA$_A$-Rs and their potential interacting proteins to investigate the targeting mechanism of GABA$_A$-Rs.

The $\alpha6\beta3\delta$ receptors were selected in this study because they are known to be present mainly at extrasynaptic sites. We first demonstrated that both $\alpha6\beta3\delta$ and $\alpha2\beta3\gamma2$-Rs were efficiently expressed on the plasma membranes of HEK cells, as shown by the surface immunostaining of the δ and $\gamma2$ subunits (Fig. 1*A*). We then examined the pharmacological characteristics of the reconstituted GABA$_A$-Rs in HEK cells. Bath application of GABA (100 μM) evoked a significant current in HEK cells expressing $\alpha6\beta3\delta$ receptors (Fig. 1*B*). Pre-application of the neurosteroid THDOC (100 nM) for 30 s significantly potentiated the GABA-evoked peak current (Fig. 1*C*, $I_{GABA} = 417 \pm 89$ pA; $I_{THDOC+GABA} = 801 \pm 169$ pA; $p < 0.001$, $n = 16$, paired t test). THIP (100 μM) induced a larger whole-cell current than that induced by 100 μM GABA (Fig. 1*D*, $I_{GABA} = 422 \pm 84$ pA; $I_{THIP} = 854 \pm 151$ pA; $p < 0.001$, $n = 17$, paired t test). These data are consistent with previous studies on neurosteroid modulation and THIP activation of δ subunit-containing GABA$_A$-Rs (45, 46). In contrast, THDOC (100 nM) negatively regulated the GABA current mediated by $\alpha2\beta3\gamma2$ receptors (Fig. 1, *E* and *F*, $I_{GABA} = 1348 \pm 195$ pA; $I_{THDOC+GABA} = 1019 \pm 173$ pA; $p < 0.001$, $n = 13$, paired t test), and THIP was a very weak agonist for $\alpha2\beta3\gamma2$ receptors (Fig. 1*G*, $I_{THIP} = 114 \pm 24$ pA; $p < 0.001$, $n = 13$, paired t test). Therefore, THDOC and THIP showed distinct pharmacological effects on $\alpha6\beta3\delta$ and $\alpha2\beta3\gamma2$ receptors.

Distinct Kinetic Properties of GABAergic Events Mediated by Different Subtypes of GABA$_A$-Rs—We previously demonstrated that NL2-transfected HEK cells receive GABAergic innervation from surrounding neurons in the HEK cell neuron co-culture system (34). Orthogonal views of Z-stack confocal images showed GABAergic terminals labeled by GAD staining (*green*) wrapping around a transfected HEK cell (Fig. 2*A*). Interestingly, GAD puncta were found not only at the bottom of the HEK cell, where the initial contact with neurons took place, but also on side and top surfaces of HEK cells. This observation suggests that following initial contact with transfected HEK cells, neuronal axons have ramified to innervate large portions of the cell surface.

We next employed patch clamp recordings to examine synaptic events in HEK cells expressing different subtypes of GABA$_A$-Rs. We found that GABA (100 μM) induced large whole-cell currents in HEK cells expressing $\alpha2\beta3$, $\alpha6\beta3$, $\alpha2\beta3\gamma2$, $\alpha6\beta3\gamma2$, or $\alpha6\beta3\delta$ receptors (Fig. 2*B*; $\alpha2\beta3$, 1158 $\pm$ 277 pA, $n = 16$; $\alpha6\beta3$, 1192 $\pm$ 295 pA, $n = 33$; $\alpha2\beta3\gamma2$, 1348 $\pm$ 195 pA, $n = 13$; $\alpha6\beta3\gamma2$, 793 $\pm$ 172 pA, $n = 9$; and $\alpha6\beta3\delta$, 417 $\pm$ 89 pA, $n = 16$). The large GABA currents coincided with the observation of synaptic like events recorded from the co-cultured HEK cells expressing these receptor subtypes (Fig. 2, *C–G*). All synaptic events in HEK cells were abolished by bicuculline (20 μM, data not shown), indicating that they were GABAergic IPSCs (34). In contrast, HEK cells expressing $\alpha2\beta3\delta$ subunits showed small whole-cell currents after bath application of 100 μM GABA (Fig. 2*B*, $\alpha2\beta3\delta$, 45 $\pm$ 23 pA, $n = 14$), and no IPSCs were detected in these cells (data not shown).

IPSCs mediated by $\alpha2\beta3$ receptors showed rapid rise and exponential decay phases, whereas IPSCs mediated by $\alpha6\beta3$ receptors showed slower rise and decay phases (Fig. 2, *C* and *D*). Thus, in the absence of the $\gamma2$ subunit, the $\alpha2\beta3$ or $\alpha6\beta3$ receptors could form functional postsynaptic structures with NL2 in HEK cells. Intriguingly, compared with the rapid rising time of IPSCs mediated by the $\alpha2\beta3\gamma2$ receptors (Fig. 2*E*), the $\alpha6\beta3\gamma2$ receptor-mediated IPSCs were also slow (Fig. 2*F*), indicating a difference between the $\alpha2$ and $\alpha6$ subunits.

The IPSCs mediated by $\alpha6\beta3\delta$ receptors showed an even slower rise phase than $\alpha6\beta3\gamma2$ IPSCs (Fig. 2*G*). The slow rise

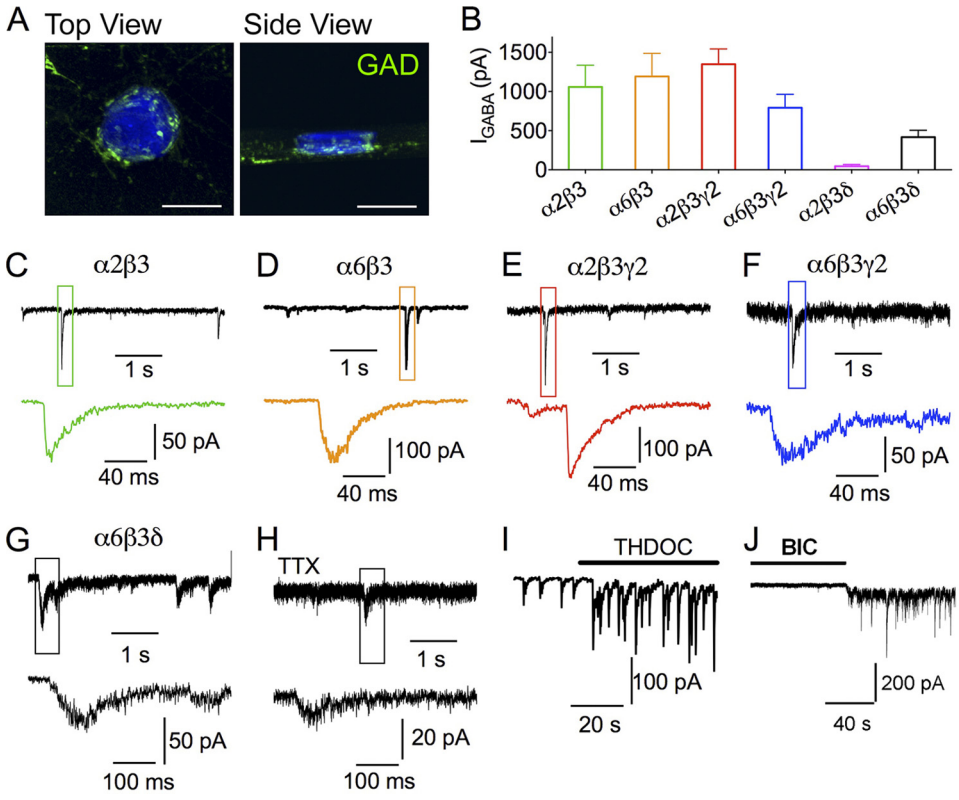

FIGURE 2. **GABA$_A$ receptors with distinct subunit combinations mediate IPSCs in HEK cells.** *A,* three-dimensional reconstitution of *Z*-stack confocal images showing the GABAergic nerve terminals (*green*) on the surface of an NL2-transfected HEK cell (*blue*). *Scale bar,* 20 μm. *B,* whole-cell currents (means ± S.E.) induced by 100 μM GABA in HEK cells expressing α2β3, α6β3, α2β3γ2, α6β3γ2, α2β3δ, and α6β3δ receptors. *C–G,* representative traces showing the IPSCs recorded in HEK cells co-expressing NL2 with α2β3 (*C*), α6β3 (*D*), α2β3γ2 (*E*), α6β3γ2 (*F*), or α6β3δ (*G*) GABA$_A$ receptors. *H,* miniature IPSCs recorded from a HEK cell expressing NL2 and α6β3δ receptors in the presence of tetrodotoxin (*TTX*) (0.5 μM). *Lower panels* show the expanded views of the *boxed* IPSCs from the *top traces*. *I,* THDOC (100 nM) increases the amplitude of IPSCs in HEK cells co-expressing α6β3δ and NL2. *J,* application of bicuculline (*BIC*) (20 μM) reduces the base-line current and the noise level, revealing the tonic current in HEK cells expressing NL2 and α6β3δ receptors.

phase of α6β3δ IPSCs was not simply due to asynchronous release of GABA from many release sites, because even in the presence of tetrodotoxin (0.5 μM), which blocks action potentials, single quantal events still showed a very slow rise phase (Fig. 2*H*). In the presence of the neurosteroid THDOC (100 nM), the amplitude of α6β3δ IPSCs was significantly increased, confirming that these events were mediated by δ subunit-containing receptors (Fig. 2*I*, median IPSC amplitude: control, 42.6 ± 7.5 pA, $n = 4$; THDOC, 92.5 ± 19.2 pA, $n = 4$; $p < 0.05$). THDOC also slightly enhanced the sIPSC frequency from 0.6 ± 0.2 Hz ($n = 4$) to 0.8 ± 0.3 Hz ($n = 4$, $p > 0.09$, not reaching statistical significance, paired *t* test). Furthermore, a tonic GABA current (~50 pA) was evident in HEK cells expressing α6β3δ receptors, as illustrated by the decreased base-line conductance and noise level in the presence of bicuculline (20 μM; Fig. 2*J*).

We next quantitatively compared the kinetics of IPSCs mediated by different GABA$_A$-Rs in HEK cells with those of IPSCs recorded from neurons (Fig. 3, *A–D*). The IPSCs recorded from α2β3γ2-expressing HEK cells showed a slightly yet significantly slower rise phase compared with neuronal IPSCs (Fig. 3, *A, B, E,* and *F*; α2β3γ2 $T_{20-80\%Rise}$ = 1.7 ± 0.2 ms, $n = 16$; neuron $T_{20-80\%Rise}$ = 1.0 ± 0.1 ms, $n = 9$; $p < 0.05$). Meanwhile, α2β3γ2 IPSCs had a typical two-exponential decay phase with a weighted time constant ($\tau_{weighted}$) significantly faster than that of neuronal IPSCs (Fig. 3*G*; neuron $\tau_{weighted}$ = 52.2 ± 5.4 ms, $n = 9$; α2β3γ2 $\tau_{weighted}$ = 29.2 ± 2.9 ms, $n = 16$; $p < 0.001$). Co-expression of gephyrin with α2β3γ2-Rs in HEK cells did not change the kinetics of IPSCs ($T_{20-80\%Rise}$ = 1.9 ± 0.3

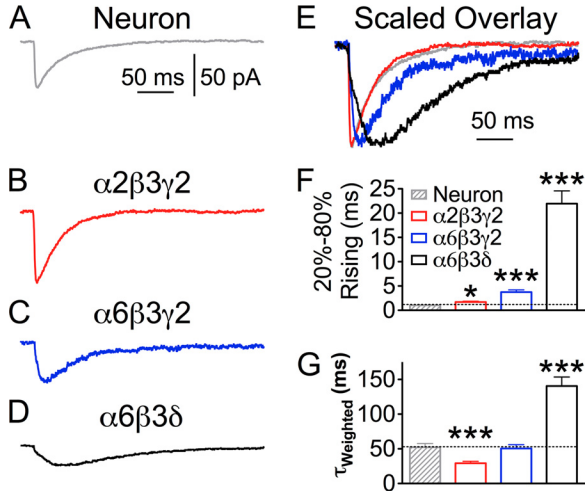

FIGURE 3. **Quantitative analysis of the kinetics of IPSCs recorded from HEK 293T cells transfected with NL2 and different sets of GABA$_A$-R subunits.** *A,* average trace of IPSCs in a neuron. *B–D,* average traces of IPSCs mediated by α2β3γ2 (*B*), α6β3γ2 (*C*), or α6β3δ (*D*) receptors. *E,* scaled overlay of IPSCs from *A–D*, showing the difference in rising and decay phases. *F* and *G,* pooled kinetics data of the IPSCs recorded from neurons and HEK cells expressing α2β3γ2, α6β3γ2, and α6β3δ receptors. *F,* 20–80% rising time, and *G,* weighted time constant ($\tau_{weighted}$) of sIPSCs. *, $p < 0.05$; ***, $p < 0.001$ (one-way ANOVA followed by Bonferroni's pairwise comparison).

ms, $n = 9$, $p > 0.5$, two-tailed t test), suggesting that gephyrin may be dispensable for the formation of hetero-synapses, or HEK cells have low levels of endogenous gephyrin (see supplemental Fig. 1). In contrast to the rapid rise phase of $\alpha2\beta3\gamma2$ IPSCs, the rise time of $\alpha6\beta3\delta$ IPSCs was an order of magnitude slower than that of neuronal IPSCs (Fig. 3, *D–G*; $T_{20-80\%\text{Rise}} = 21.9 \pm 2.6$ ms; $\tau_{\text{weighted}} = 140.6 \pm 12.8$ ms; $n = 13$; $p < 0.001$). The very slow rise phase was consistent with slow IPSCs previously observed in cerebellar granule cells, which are mediated by $\alpha6$ subunit-containing GABA$_A$-Rs localized far from GABA release sites (47). Our data suggest that $\alpha6\beta3\delta$ receptors assume an extrasynaptic localization, whereas $\alpha2\beta3\gamma2$ receptors cluster at synaptic sites in the hetero-synapse model.

Interestingly, the rise phase of $\alpha6\beta3\gamma2$ IPSCs was significantly faster than that of $\alpha6\beta3\delta$ IPSCs, yet significantly slower than that of $\alpha2\beta3\gamma2$ IPSCs (Fig. 3 *C, E* and *F*; $T_{20-80\%\text{Rise}}$: $\alpha6\beta3\gamma2 = 3.7 \pm 0.4$ ms, $n = 9$; $\alpha6\beta3\gamma2$ *versus* $\alpha6\beta3\delta$, $p < 0.001$; $\alpha6\beta3\gamma2$ *versus* $\alpha2\beta3\gamma2$, $p < 0.001$; Bonferroni's multiple comparison test). In addition, IPSCs mediated by $\alpha6\beta3$ receptors showed significantly slower rise phase than the events mediated by $\alpha2\beta3$ receptors ($T_{20-80\%\text{Rise}}$: $\alpha6\beta3$, 5.1 ± 1.0, $n = 8$; $\alpha2\beta3$, 2.2 ± 0.3 ms, $n = 11$; **, $p < 0.01$, two-tailed t test). Notably, there is no significant difference between the rise phase of IPSCs mediated by $\alpha2\beta3$ and $\alpha2\beta3\gamma2$ receptors ($p > 0.1$) nor between $\alpha6\beta3$ and $\alpha6\beta3\gamma2$ receptors ($p > 0.1$). These results indicate that distinct α subunits play a significant role in shaping GABAergic responses.

Rapid Onset Kinetics of GABA$_A$-Rs Composed of Different Subunits—We wondered whether the onset kinetics of different receptors might explain such a drastic difference in the IPSC rise phases. To answer this question, we employed a high speed solution exchange system to apply GABA (10 mM) to outside-out patches excised from transfected HEK cells (Fig. 4*A*). Ultrafast GABA application was achieved by starting GABA perfusion and stopping bath solution simultaneously. We found that $\alpha2\beta3\gamma2$-Rs were activated rapidly upon GABA application (Fig. 4, *B* and *G*, $T_{20-80\%\text{Rise}} = 1.0 \pm 0.2$ ms, $n = 8$), faster than the rise phase of $\alpha2\beta3\gamma2$-mediated IPSCs in HEK cells but comparable with neuronal IPSCs. This result suggests that GABA$_A$ receptors in HEK cells are not clustered as tightly as in neuronal cells. The rise phase of $\alpha6\beta3\gamma2$-Rs was indistinguishable from that of $\alpha2\beta3\gamma2$-Rs (Fig. 4, *B* and *G*, $T_{20-80\%\text{Rise}}$: $\alpha6\beta3\gamma2 = 1.0 \pm 0.2$ ms, $n = 8$; $p > 0.9$). However, the rise phase of $\alpha6\beta3\delta$-mediated GABA currents was significantly slower than that of $\alpha2\beta3\gamma2$ or $\alpha6\beta3\gamma2$ receptors (Fig. 4, *B* and *G*, $T_{20-80\%\text{Rise}}$: $\alpha6\beta3\delta = 2.3 \pm 0.3$ ms, $n = 10$; $p < 0.01$ for both comparisons, one-way ANOVA followed by Bonferroni's pairwise comparison), yet it was still an order of magnitude faster than that of $\alpha6\beta3\delta$-IPSCs in HEK cells. Because the difference in receptor kinetics is too small to explain the drastic 10-fold difference between the rise phase of $\alpha2\beta3\gamma2$ and $\alpha6\beta3\delta$ IPSCs, the slow $\alpha6\beta3\delta$-IPSCs is likely a result of the extrasynaptic localization of $\alpha6\beta3\delta$ receptors.

Ultrastructural Localization of GABA$_A$-Rs—We further carried out immunoelectron microscopic studies to reveal the ultrastructural localization of $\alpha6\beta3\delta$ and $\alpha2\beta3\gamma2$ receptors in neuron-HEK cell co-cultures. HEK cells expressing $\alpha6\beta3\delta$ or $\alpha2\beta3\gamma2$ receptors were identified by silver-enhanced gold particles immunolabeling the δ or $^{myc}\gamma2$ subunit. Nerve terminals containing synaptic vesicles were found in close contact with HEK cells. Importantly, gold particles immunopositive for δ receptors were localized mostly at extrasynaptic membranes, whereas $\gamma2$-positive particles were mainly at synaptic cleft (Fig. 5, *A* and *B*). To quantify the detailed receptor localization, 7 randomly selected sections with a total of 34 synapses and 55 gold particles labeling δ-receptors were analyzed. The majority of particles (80%) were localized at extrasynaptic membranes, whereas only 12.7 and 7.3% were localized perisynaptically or synaptically (Fig. 5*C*). For comparison, 6 sections containing 18 synapses from $\alpha2\beta3\gamma2$-expressing HEK cells were assessed. Among 81 $\gamma2$-immunoreactive particles analyzed, 63% were synaptic and 16% perisynaptic, with the remaining 21% being extrasynaptic (Fig. 5*C*). The immuno-EM results confirmed

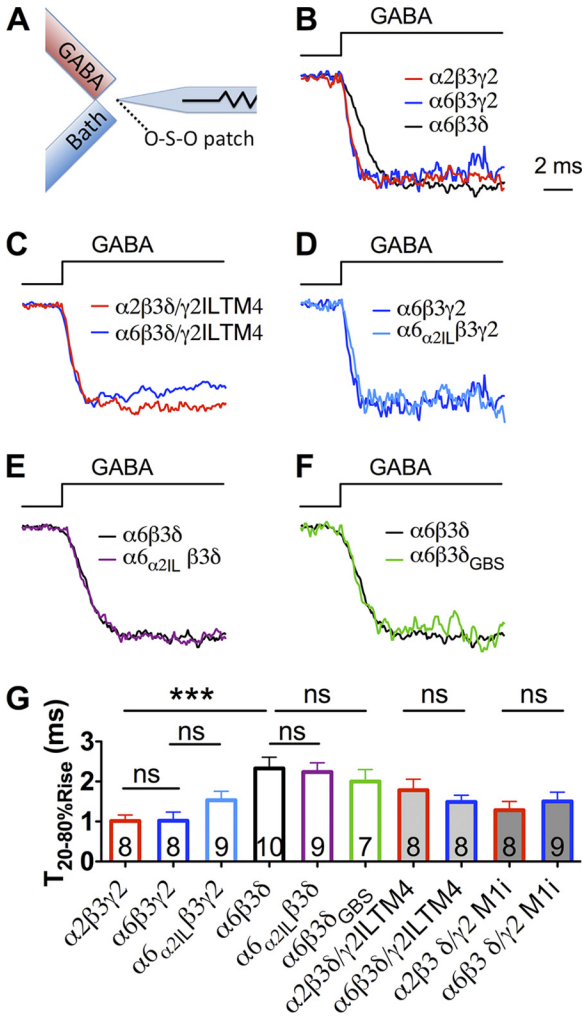

FIGURE 4. **Onset kinetics of recombinant GABA$_A$-Rs.** *A*, schematic diagram illustrating the fast drug application system. Fast GABA application was achieve by starting the GABA perfusion and stopping the flow of bath solution instantaneously. *B–F*, representative traces of GABA-induced currents on outside-out patches excised from transfected HEK cells. *B*, rise time of $\alpha6\beta3\delta$-Rs was slower than that of $\alpha2\beta3\gamma2$- and $\alpha6\beta3\gamma2$-Rs. *C*, no significant difference in the onset kinetics when substituting the $\alpha2$ with $\alpha6$ subunit in $\delta/\gamma2$IL-TM4 chimeric receptors. *D* and *E*, insertion of $\alpha2$IL into the $\alpha6$ subunit ($\alpha6_{\alpha2\text{IL}}$) did not change the onset kinetics of $\alpha6$-containing receptors. *F*, insertion of the GBS into the δ subunit (δ_{GBS}) did not change the onset kinetics of the $\alpha6\beta3\delta$ receptors. *G*, polled data showing the 20–80% rise time of each recombinant GABA$_A$-R. ***, $p < 0.001$ (one-way ANOVA followed by Bonferroni's pairwise comparison). *ns*, no significance.

that the $\alpha6\beta3\delta$ GABA$_A$-Rs are preferentially localized at extrasynaptic membranes in the hetero-synapse model. Together with the kinetics analysis (Figs. 2–4), the IPSC rise phase seems to be a faithful indicator of receptor localization in our hetero-synapse model; fast rise phase indicates synaptic localization, and slow rise phase indicates extrasynaptic or perisynaptic localization.

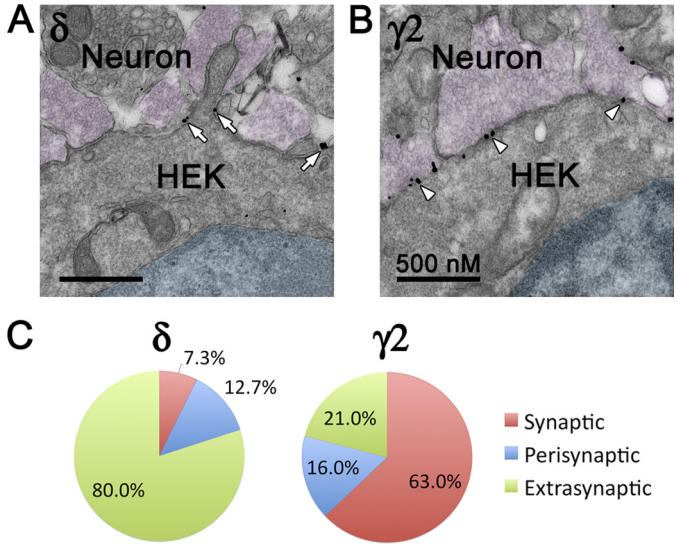

FIGURE 5. **Ultrastructural localization of $\alpha6\beta3\delta$- and $\alpha2\beta3\gamma2$-GABA$_A$-Rs in the hetero-reconstituted synapses.** *A* and *B,* transfected HEK cells in close contact with nerve terminals. The nuclei of HEK cells are *shaded cyan*. Nerve terminals containing synaptic vesicles are shown in *magenta*. *A,* $\alpha6\beta3\delta$ receptors were predominantly localized at extrasynaptic or perisynaptic membranes. *Arrows,* silver-enhanced gold particles labeling the δ subunit-containing receptors. *B,* $\alpha2\beta3\gamma2$ receptors were mainly localized at synaptic sites. *Arrowheads,* immunogold labeling of the GFP-γ2 subunit. *C, pie graphs* showing the percentage of synaptic, perisynaptic, and extrasynaptic labeling in HEK cells expressing $\alpha6\beta3\delta$ or $\alpha2\beta3\gamma2$ receptors.

α2 and α6 Subunits Directly Target Chimeric Receptors to Synaptic and Extrasynaptic Sites—Given the significant difference in the rise phase of $\alpha2\beta3$ *versus* $\alpha6\beta3$ IPSCs and $\alpha2\beta3\gamma2$ *versus* $\alpha6\beta3\gamma2$ IPSCs (Figs. 2 and 3), we hypothesized that α2 and α6 subunits play a distinctive role in receptor targeting. To test this hypothesis, a series of δ/γ2 chimeras were co-expressed with either α2 or α6 subunits, together with β3 subunit and NL2 in HEK cells. Fig. 6*A* illustrates the domain compositions of the δ/γ2 chimeras. Interestingly, when different δ/γ2 chimeras were combined with α2 and β3 subunits, they all mediated fast rising IPSCs (Fig. 6*B*, *black traces*). In contrast, when combined with α6 and β3 subunits, these chimeras all yielded slow IPSCs (Fig. 6*B*, *gray traces*). Importantly, for each individual δ/γ2 chimera, the IPSC rise phase was always slower when it was co-assembled with the α6 compared with the α2 subunit (Fig. 6*C* and supplemental Table 1). Similarly, the decay phase of the IPSCs mediated by each δ/γ2 chimera was always slower when co-expressed with the α6 subunit (Fig. 6*D*). Fig. 6*E* shows large GABA-induced whole-cell currents in HEK cells expressing all different chimeric receptors.

The onset kinetics of receptors containing δ/γ2ILTM4 and δ/γ2 M1i were analyzed as well (Fig. 4, *C* and *G*). Interestingly, different α subunits (α2 *versus* α6) did not change the receptor onset kinetics ($\alpha2\beta3\delta/\gamma2_{ILTM4}$, $T_{20-80\%Rise} = 1.8 \pm 0.3$ ms, $n = 8$; $\alpha6\beta3\delta/\gamma2_{ILTM4}$, $T_{20-80\%Rise} = 1.5 \pm 0.2$ ms, $n = 8$; $p > 0.3$; $\alpha2\beta3\delta/\gamma2$ M1i, $T_{20-80\%Rise} = 1.3 \pm 0.2$ ms, $n = 8$; $\alpha6\beta3\delta/\gamma2$ M1i, $T_{20-80\%Rise} = 1.5 \pm 0.2$ ms, $n = 9$; $p > 0.5$). Therefore, the difference in IPSC rise phase mediated by these chimeric recep-

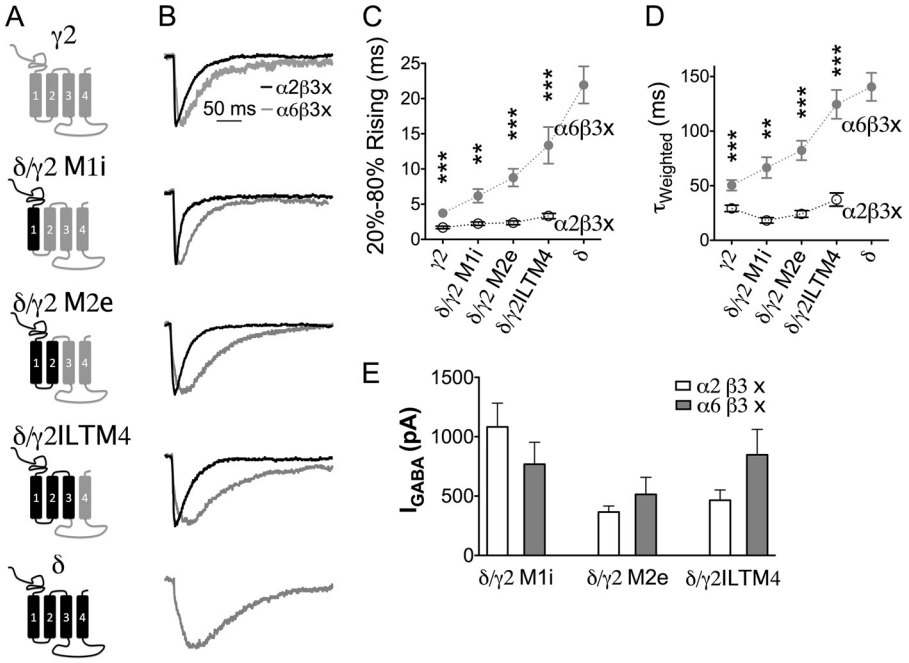

FIGURE 6. **Different α subunits contribute to the distinct kinetics of sIPSCs.** *A,* schematic representation of a series of δ/γ2 chimeric subunits. *IL,* intracellular loop; *TM,* transmembrane domain. *B,* average traces of sIPSCs recorded from representative HEK cells expressing γ2 subunits, δ subunits, or δ/γ2 chimeras together with either α2 and β3 or α6 and β3 subunits and NL2 "x" in a2b3x or a6b3x stands for either g2, d, or their chimeric subunit. *C,* pooled data (mean ± S.E.) showing the 20–80% rise time of IPSCs in HEK cells expressing different subunit combinations. Each chimera showed significantly faster rise phase when paired up with the α2 subunit, compared with when the α6 subunit was their assembly partner. **, $p < 0.01$; ***, $p < 0.001$, two-tailed *t* test. *D,* average weighted time constant ($\tau_{weighted}$) of sIPSCs mediated by different subunit combinations (mean ± S.E.). *E,* GABA-induced current (100 μM) mediated by δ/γ2 chimera-containing receptors in HEK cells.

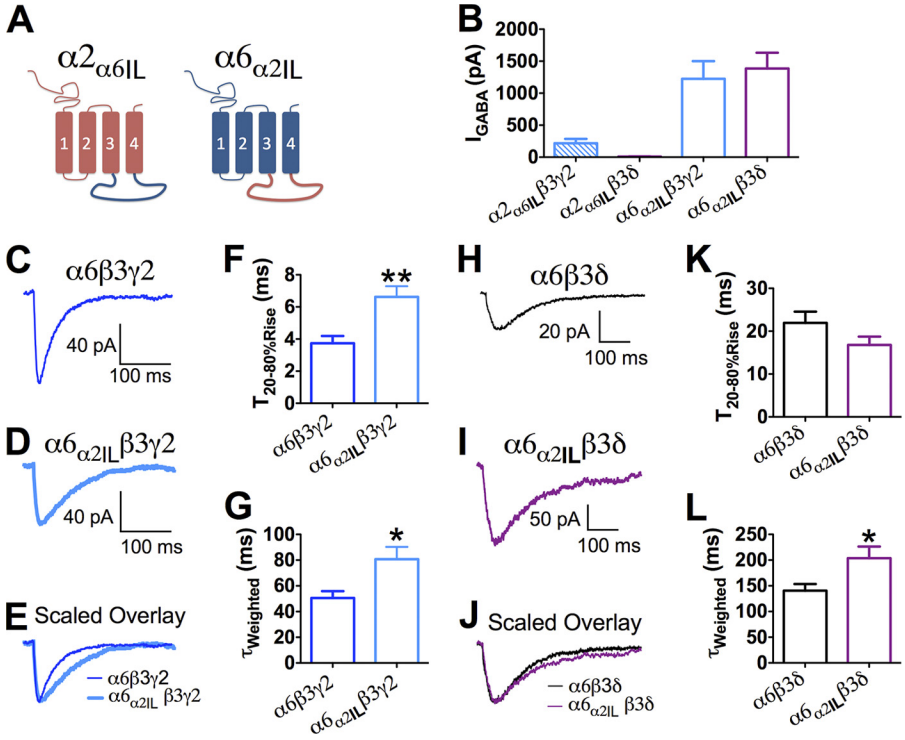

FIGURE 7. **α2 subunit intracellular domain was not sufficient to determine synaptic receptor targeting.** *A*, schematic diagram indicating the structure of $\alpha2_{\alpha6IL}$ and $\alpha6_{\alpha2IL}$ chimeras. *B*, whole-cell current induced by 100 μM GABA in HEK cells expressing $\alpha2_{\alpha6IL}\beta3\gamma2$, $\alpha2_{\alpha6IL}\beta3\delta$, $\alpha6_{\alpha2IL}\beta3\gamma2$, and $\alpha6_{\alpha2IL}\beta3\delta$ receptors. *C* and *D*, averaged sIPSC traces recorded from HEK cells expressing $\alpha6\beta3\gamma2$ or $\alpha6_{\alpha2IL}\beta3\gamma2$ receptors. *E*, scaled overlay of $\alpha6\beta3\gamma2$ or $\alpha6_{\alpha2IL}\beta3\gamma2$ receptor-mediated IPSCs. *F* and *G*, pooled data (mean ± S.E.) showing the comparison of the 20–80% rising and $\tau_{weighted}$ of $\alpha6\beta3\gamma2$ and $\alpha6_{\alpha2IL}\beta3\gamma2$ receptor-mediated IPSCs. *H* and *I*, representative traces showing the averaged sIPSC events from HEK cells expressing $\alpha6\beta3\delta$ (*H*) and $\alpha6_{\alpha2IL}\beta3\delta$ (*I*) receptors. *J*, scaled overlay of $\alpha6\beta3\delta$ or $\alpha6_{\alpha2IL}\beta3\delta$ receptor-mediated IPSCs. *K* and *L*, pooled data comparing the 20–80% rising and $\tau_{weighted}$ of $\alpha6\beta3\delta$ and $\alpha6_{\alpha2IL}\beta3\delta$ receptor-mediated IPSCs. *, $p < 0.05$; **, $p < 0.01$

tors shown in Fig. 6 was likely caused by distinct receptor localization. Thus, the same δ/γ2 chimera can be targeted to either synaptic sites if co-assembled with the α2 subunit or targeted to extrasynaptic sites if co-assembled with the α6 subunit. These results suggest that different α subunits play a direct role in guiding receptor localization.

We then explored the structural differences between α2 and α6 subunits that might contribute to differential receptor targeting. The intracellular loop of the α2 subunit has been found to interact with gephyrin, a scaffolding protein at inhibitory synapses to stabilize GABA$_A$-R clusters (48). To test the role of the intracellular loop in receptor targeting, we swapped the intracellular loop of α2 and α6 subunits, generating chimeras $\alpha2_{\alpha6IL}$ and $\alpha6_{\alpha2IL}$ (Fig. 7*A*). The $\alpha6_{\alpha2IL}$ chimera was capable of forming functional GABA$_A$-Rs efficiently with either β3γ2 or β3δ subunits, as indicated by large GABA-induced whole-cell currents in transfected HEK cells (Fig. 7*B*; $\alpha6_{\alpha2IL}\beta3\gamma2$, I_{GABA} = 1224.0 ± 277.5 pA, $n = 11$; $\alpha6_{\alpha2IL}\beta3\delta$, I_{GABA} = 1385.0 ± 246.7 pA, $n = 29$). By contrast, the $\alpha2_{\alpha6IL}$ subunit-containing receptors showed very small GABA-induced current when expressed in HEK cells (Fig. 7*B*; $\alpha2_{\alpha6IL}\beta3\gamma2$, I_{GABA} = 217.1 ± 68.6 pA, n = 22; $\alpha2_{\alpha6IL}\beta3\delta$, I_{GABA} = 9.4 ± 2.8 pA, $n = 14$), making it impossible to assay postsynaptic events mediated by these receptors. We therefore focused on the $\alpha6_{\alpha2IL}$ construct.

The IPSCs mediated by $\alpha6_{\alpha2IL}\beta3\gamma2$ and $\alpha6_{\alpha2IL}\beta3\delta$ receptors were compared with those mediated by receptors containing the wild type α6 subunit (α6β3γ2 and α6β3δ). Unexpectedly, the $\alpha6_{\alpha2IL}\beta3\gamma2$ IPSCs showed slower rise and decay phases than wild type α6β3γ2 IPSCs (Fig. 7, *F* and *G*, $\alpha6_{\alpha2IL}\beta3\gamma2$, $T_{20-80\%\ Rise}$ = 6.6 ± 0.7 ms, $\tau_{weighted}$ = 80.7 ± 9.6 ms, $n = 10$; α6β3γ2 $T_{20-80\%Rise}$ = 3.7 ± 0.4 ms, $p < 0.01$, $\tau_{weighted}$ = 50.6 ± 5.3 ms, $p < 0.05$,). As for the $\alpha6_{\alpha2IL}\beta3\delta$ IPSCs, the rise phase was not different from that of α6β3δ IPSCs (Fig. 7*K*; $\alpha6_{\alpha2IL}\beta3\delta$, 16.8 ± 2.0 ms, $n = 13$; α6β3δ 21.9 ± 2.6 ms, $n = 13$; $p > 0.1$), but the decay time constant of $\alpha6_{\alpha2IL}\beta3\delta$ IPSCs was increased by 45% compared with that of α6β3δ IPSCs (Fig. 7*L*; $\alpha6_{\alpha2IL}\beta3d$, $\tau_{weighted}$ = 203.7 ± 22.7 ms, n = 13; α6β3δ, $\tau_{weighted}$ = 140.6 ± 12.8 ms, $n = 13$; $p < 0.05$). Our results showed that substitution of the α2 IL in the α6 subunit did not generate faster IPSCs, suggesting that the α2 IL domain alone cannot direct GABA$_A$-Rs to synaptic sites.

The onset kinetics of $\alpha6_{\alpha2IL}$-containing receptors was similar to those of receptors containing the wild type α6 subunit (Fig. 4, *D*, *E*, and *G*). The 20–80% rise time of GABA-induced currents was 1.5 ± 0.2 ms for the $\alpha6_{\alpha2IL}\beta3\gamma2$-Rs ($n = 9$, $p > 0.1$ compared with α6β3γ2-Rs) and 2.2 ± 0.2 ms for the $\alpha6_{\alpha2IL}\beta3\delta$-Rs ($n = 9$, $p > 0.8$ compared with α6β3δ-Rs).

Recruiting α6β3δ GABA$_A$-Rs to Synaptic Sites through Forced Interaction with Gephyrin—Gephyrin is known to cluster at inhibitory synapses, where it stabilizes synaptic GABA$_A$-Rs (28, 40, 49–54). We wondered whether enhancing gephyrin interaction with α6β3δ receptors can target them to synaptic sites. Therefore, we modified the intracellular loop of α6 and δ subunits by insertion of a gephyrin-binding site (GBS) derived from the glycine receptor β subunit, generating $\alpha6_{GBS}$ and δ_{GBS} chimeras (Fig. 8*A*). The interaction between δ_{GBS} and gephyrin was demonstrated by co-immunoprecipitation assay (Fig. 8*B*). The δ_{GBS} and $\alpha6_{GBS}$ subunits were also co-expressed with gephyrin-GFP in HEK cells to examine their co-localization.

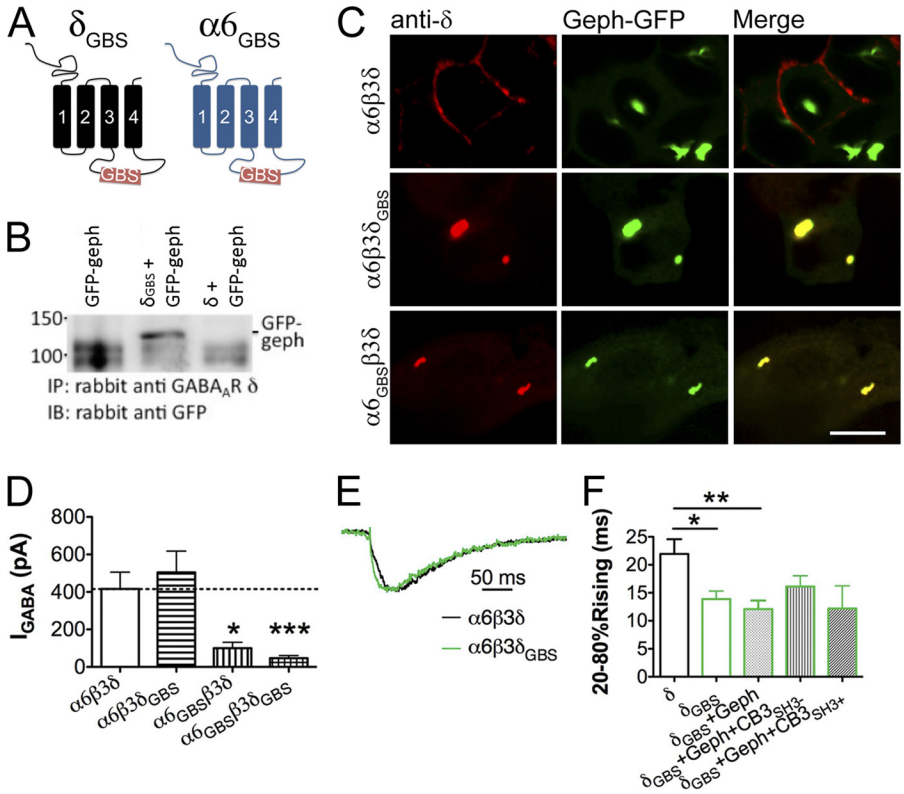

FIGURE 8. **Interaction with gephyrin targets α6β3δ-containing GABA$_A$-Rs to synaptic sites of reconstituted synapses.** *A*, schematic representation of the δ_{GBS} and $\alpha6_{GBS}$ chimeras. *B*, GFP-gephyrin (*geph*) was co-precipitated with the δ_{GBS} chimera. *C*, $\alpha6\beta3\delta_{GBS}$ and $\alpha6_{GBS}\beta3\delta$ receptors were found to co-localize with gephyrin-GFP in big intracellular aggregates when co-expressed in HEK cells, demonstrating the interaction between δ_{GBS} and $\alpha6_{GBS}$ subunits and gephyrin; $\alpha6\beta3\delta$ receptors showed no co-localization with gephyrin-GFP. *Scale bar*, 10 μm. *D*, whole-cell GABA current in HEK cells expressing the δ_{GBS} and/or $\alpha6_{GBS}$ chimeras. *E*, sample traces of sIPSCs mediated by $\alpha6\beta3\delta$ or $\alpha6\beta3\delta_{GBS}$ receptors. The events were scaled to the same amplitude and aligned according to the initial rise time. *F*, pooled data of sIPSC rise time in different groups. The $\alpha6\beta3\delta_{GBS}$ receptor-mediated sIPSCs showed a rise phase significantly faster than that of $\alpha6\beta3\delta$ receptors. Co-expression of gephyrin or gephyrin plus collybistin did not further change the IPSC rise time. *, $p < 0.05$; **, $p < 0.01$; ***, $p < 0.001$ (one-way ANOVA followed by Bonferroni's pairwise comparison).

Gephyrin-GFP tends to form large intracellular aggregates when overexpressed in HEK cells (Fig. 8*C*). Both $\alpha6\beta3\delta_{GBS}$ and $\alpha6_{GBS}\beta3\delta$ receptors co-localized with gephyrin aggregates, whereas the wild type $\alpha6\beta3\delta$ receptors did not (Fig. 8*C*). Thus, our newly constructed δ_{GBS} and $\alpha6_{GBS}$ subunits interact with gephyrin as predicted.

The whole-cell GABA current in cells expressing $\alpha6\beta3\delta_{GBS}$ receptors was similar to that of $\alpha6\beta3\delta$ receptor-expressing cells, whereas $\alpha6_{GBS}\beta3\delta$ and $\alpha6_{GBS}\beta3\delta_{GBS}$ receptors showed a very small GABA-induced current (Fig. 8*D*; I_{GABA}: $\alpha6\beta3\delta$, 417 ± 89 pA, $n = 16$; $\alpha6\beta3\delta_{GBS}$, 504 ± 113 pA, $n = 20$; $\alpha6_{GBS}\beta3\delta$, 100 ± 32 pA, $n = 6$, $p < 0.05$; $\alpha6_{GBS}\beta3\delta_{GBS}$, 47 ± 14 pA, $n = 6$, $p < 0.001$). Thus, we focused on analyzing the IPSCs mediated by $\alpha6\beta3\delta_{GBS}$ GABA$_A$-Rs. As shown in Fig. 8*E*-F, $\alpha6\beta3\delta_{GBS}$ receptor-mediated IPSCs had a significantly faster rise phase compared with those mediated by $\alpha6\beta3\delta$ receptors ($\alpha6\beta3\delta_{GBS}$, $T_{20-80\%Rise}$ = 13.9 ± 1.4 ms, $n = 8$; $\alpha6\beta3\delta$, $T_{20-80\%Rise}$ = 21.9 ± 2.6 ms, $n = 13$; $p < 0.05$). Interestingly, co-expression of gephyrin with $\alpha6\beta3\delta_{GBS}$-Rs did not shorten the IPSC rise time (Fig. 8*F*, $\alpha6\beta3\delta_{GBS}$ + gephyrin, $T_{20-80\%Rise}$ = 12.1 ± 1.5 ms, $n = 10$, $p > 0.4$ compared with $\alpha6\beta3\delta_{GBS}$). Similarly, further addition of collybistin ($CB3_{SH3-}$ or $CB3_{SH3+}$ (41)) resulted in sIPSCs with rising time similar to that of $\alpha6\beta3\delta_{GBS}$ alone (Fig. 8*F*, $\alpha6\beta3\delta_{GBS}$ + gephyrin + $CB3_{SH3-}$ *versus* $\alpha6\beta3\delta_{GBS}$, $p > 0.3$; $\alpha6\beta3\delta_{GBS}$ + gephyrin + $CB3_{SH3+}$ *versus* $\alpha6\beta3\delta_{GBS}$, $p > 0.6$). These results suggest that insertion of the gephyrin binding domain brought the $\alpha6\beta3\delta_{GBS}$ receptors closer to postsynaptic sites, possibly through the interaction with endogenous gephyrin in HEK cells (supplemental Fig. 1). Our kinetics analysis revealed that the $\alpha6\beta3\delta_{GBS}$-Rs (co-expressed with gephyrin and $CB3_{SH3-}$) responded to GABA application at a rate similar to $\alpha6\beta3\delta$-Rs (Fig. 4, *F* and *G*, $\alpha6\beta3\delta_{GBS}$ $T_{20-80\%Rise}$ = 2.0 ± 0.3 ms, $n = 7$, $p > 0.4$), indicating that the insertion of GBS did not change the receptor kinetics.

The targeting of $\alpha6_{GBS}$ and δ_{GBS} subunits was further analyzed in neurons co-transfected with $\alpha6_{GBS}$, $\beta3$, and δ_{GBS} subunits. Transfected neurons were double immunolabeled to visualize the co-localization of the δ subunit and gephyrin or the δ subunit and GAD. As control, neurons transfected with $\alpha6\beta3\delta$ or $\alpha2\beta3\gamma2$ were also examined. We found that δ subunit-containing receptors were diffusely localized throughout the neuronal membrane surface, without obvious enrichment at synaptic sites apposed to GAD-labeled presynaptic terminals (Fig. 9*A*). By contrast, the immunostaining of the γ2 subunit revealed punctate labeling along the dendrites, with many clusters juxtaposed to GAD puncta (Fig. 9*B*). Intriguingly, neurons overexpressing δ_{GBS}-containing receptors showed punctate staining, which was also co-localized with punctate gephyrin staining (Fig. 9*C*). More importantly, some of the δ_{GBS}-containing puncta were found jux-

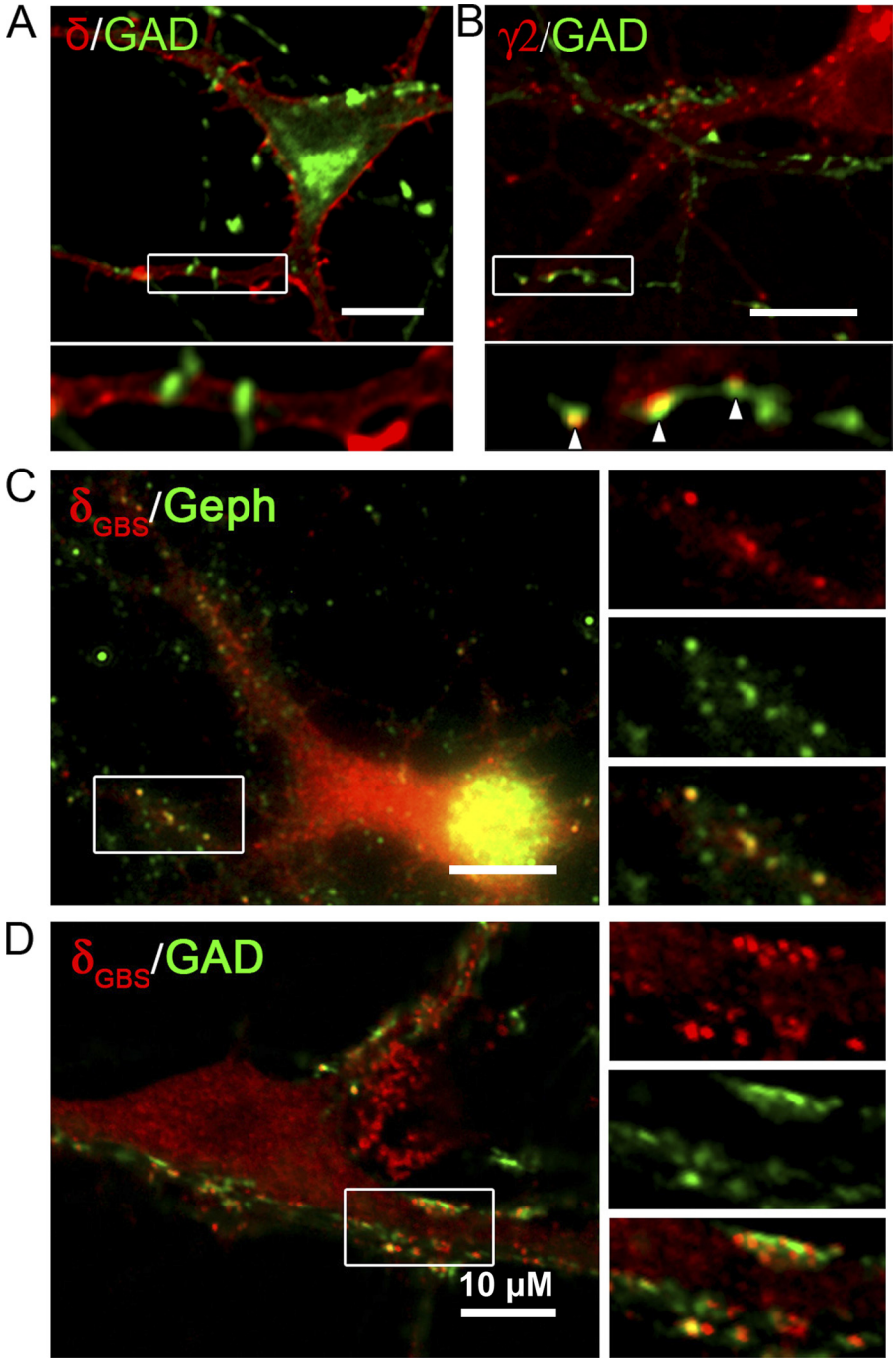

FIGURE 9. **Incorporation of the gephyrin-binding site induces clustering of $\alpha6\beta3\delta$-receptors at postsynaptic sites in neurons.** *A,* hypothalamic neurons co-transfected with $\alpha6$, $\beta3$, and δ subunits were double immunolabeled for the δ subunit and GAD. Immunoreactivity for the δ subunit was diffusely localized on the neuronal surface. *B,* neurons were co-transfected with $\alpha2$, $\beta3$, and $^{myc}\gamma2$ subunits, followed by GAD and surface $^{myc}\gamma2$ double staining. The $\gamma2$ subunit-containing receptors formed puncta along the dendrites, some of which were apposed to GAD puncta. *C* and *D,* neurons transfected with $\alpha6_{GBS}$, $\beta3$, and δ_{GBS} subunits were double immunolabeled for the δ_{GBS} subunit and gephyrin (*Geph*) (*C*) or δ_{GBS} and GAD (*D*). The δ_{GBS} subunit-containing receptors formed clusters in neurons. A portion of the δ_{GBS} subunit-containing receptors were co-localized with gephyrin clusters (*right panels* in *C*) or with GAD puncta (*right panels* in *D*), suggesting a synaptic localization.

taposed to GAD puncta (Fig. 9*D*), suggesting that these GBS-containing chimeric receptors were recruited to postsynaptic sites in neurons, likely through interaction with gephyrin.

DISCUSSION

In this study, we demonstrate that different subtypes of $GABA_A$-Rs are distinctly targeted to synaptic and extrasynaptic sites in neuron-HEK cell hetero-synapses. With this unique synapse model, we found that $\alpha2$ and $\alpha6$ subunits target the same $\delta/\gamma2$ chimeric subunit to synaptic and extrasynaptic sites, respectively, suggesting a direct role of α subunits in $GABA_A$-R targeting. Furthermore, forced interaction of the $\alpha6$ or δ subunit with gephyrin can recruit normally extrasynaptic $\alpha6\beta3\delta$ receptors closer to synaptic sites, suggesting that gephyrin can stabilize any interactive $GABA_A$-Rs at synaptic sites. Fig. 10 is a schematic diagram illustrating the relative subcellular localiza-

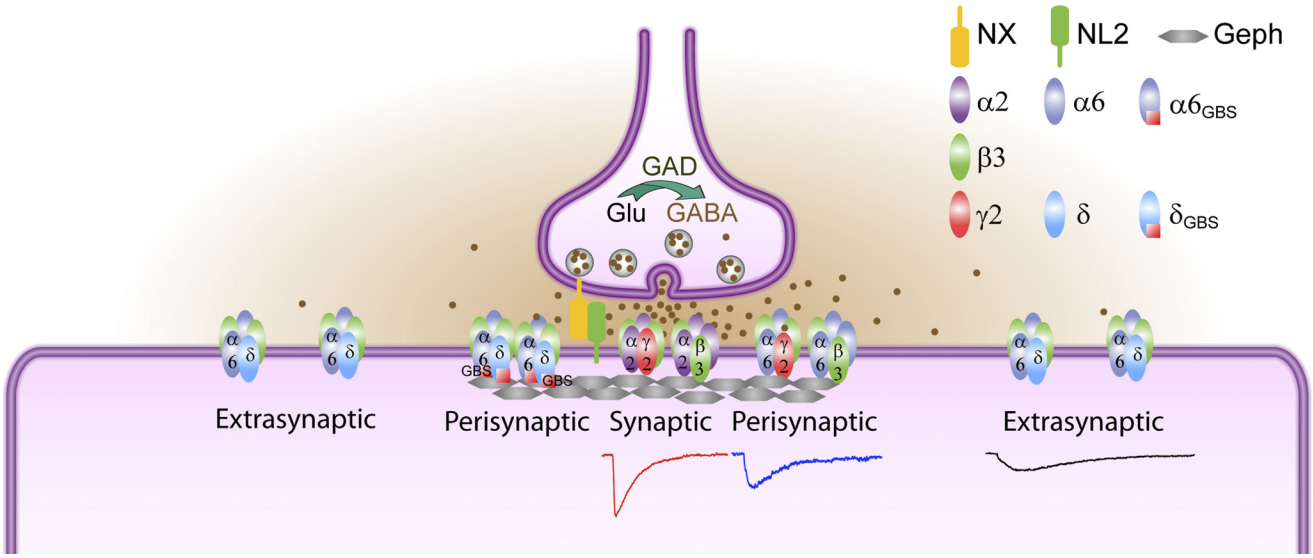

FIGURE 10. **Model for synaptic *versus* extrasynaptic GABA$_A$-R targeting.** The $\alpha2\beta3$ and $\alpha2\beta3\gamma2$ GABA$_A$-Rs are clustered at synaptic sites, mediating fast IPSCs. The $\alpha6\beta3\delta$ GABA$_A$-Rs are localized at extrasynaptic sites, mediating very slow IPSCs, which may be partly due to a lack of binding with gephyrin (*Geph*). Importantly, the $\alpha6\beta3$ and $\alpha6\beta3\gamma2$ GABA$_A$-Rs are likely localized at perisynaptic sites, resulting in IPSC kinetics in-between that of $\alpha2\beta3\gamma2$ and $\alpha6\beta3\delta$ GABA$_A$-Rs. The $\alpha6_{GBS}\beta3\delta_{GBS}$ GABA$_A$-Rs are brought closer to synaptic sites.

tions of different subtypes of GABA$_A$-Rs investigated in this study. Importantly, the intermediate rise and decay phases of $\alpha6\beta3$- and $\alpha6\beta3\gamma2$-IPSCs suggest that these receptors are most likely localized at perisynaptic sites, different from the synaptic $\alpha2\beta3\gamma2$ or extrasynaptic $\alpha6\beta3\delta$ receptors. Such distinct IPSC events with graded changes of rise and decay phases are difficult to distinguish in neurons, underscoring the advantage of our model synapses in pinpointing the precise targeting mechanisms of specific subtype receptors.

Molecularly Engineered Synapses as a Model System to Study Receptor Targeting—The hetero-co-culture system is often used to study synaptogenesis induced by cell adhesion molecules, such as neuroligins, SynCAM, netrin-G ligand, and LRRTM (39, 55–61). We have previously shown that functional GABAergic synapses can be formed in HEK 293T cells by co-expressing NL2 and $\alpha2\beta3\gamma2$ GABA$_A$-Rs (34). Here, we further developed the hetero-synapses as a model system to study GABA$_A$-R targeting. The advantage of this system is the precise control of the expression of specific receptor subtypes, avoiding the complexity of GABA$_A$-Rs in neurons. For example, if a neuron contains both $\alpha2\beta3\gamma2$ and $\alpha6\beta3\gamma2$ receptors, it will be difficult to know whether recorded IPSCs are mediated by $\alpha2\beta3\gamma2$ or $\alpha6\beta3\gamma2$ receptors or both. Our model synapses offer clear distinction between synaptic events mediated by $\alpha2\beta3\gamma2$ and $\alpha6\beta3\gamma2$ receptors (Fig. 3), providing an important research tool for future studies on different subtypes of receptors. Furthermore, we have recently demonstrated that such a model system is useful for the screening of human disease-related gene mutations by co-expressing GABA$_A$-Rs with wild type or mutant NL2 identified from patients with schizophrenia (62). Our previous and current studies suggest that molecularly engineered hetero-synapses are a versatile model system that can be used to study not only synaptogenesis but also receptor targeting and functional deficits of gene mutations.

α Subunits Are Sufficient to Target GABA$_A$-Rs—Previous studies suggest that γ2 subunit-containing GABA$_A$-Rs are mainly concentrated at postsynaptic sites (28–30), whereas δ subunit-containing GABA$_A$-Rs are mostly distributed in extrasynaptic membranes (2, 5, 7, 8, 31, 63). Based on the present analyses of δ/γ2 chimeras, it seems that there is no single domain in the δ subunit responsible for the slow IPSC kinetics, because the rise phases became increasingly slower with chimeras containing a greater portion of the δ subunit (Fig. 6*B*). As for the role of different α subunits, recent studies found that targeted deletion of α1, α2, or α3 subunit abolishes γ2-containing postsynaptic receptor clusters in selective subcellular regions (24–27). Conversely, deletion of α4, α5, or α6 subunit greatly reduced tonic currents, suggesting an extrasynaptic localization (64–66). These knock-out experiments suggest that the α subunit is required for functional assembly of synaptic (α1–3)- and extrasynaptic (α4–6)- GABA$_A$-Rs, but they did not address whether the α subunit is involved in receptor targeting.

In this work, we directly investigated the role of α2 and α6 subunits in GABA$_A$-R targeting. We first observed a slower rise phase of $\alpha6\beta3\gamma2$-IPSCs than that of $\alpha2\beta3\gamma2$-IPSCs. Similarly, $\alpha6\beta3$-IPSCs were also slower than $\alpha2\beta3$-IPSCs, a clear indication of differential functions of the two α subunits. The direct role of the α subunit in receptor targeting was discovered by co-assembling with a series of δ/γ2 chimeras. We demonstrated that when combined with the α2 subunit, the δ/γ2 chimeras always mediated fast IPSCs, similar to that mediated by synaptic γ2-containing receptors; but when combined with the α6 subunit, the same δ/γ2 chimeras always mediated very slow IPSCs, reminiscent of that by extrasynaptic δ-containing receptors (Fig. 6). Because the α2 and α6 subunits do not affect the onset kinetics of GABA$_A$-Rs (Fig. 4), the drastic difference in IPSC rise phase likely reflects the difference in receptor localization. Thus, the same δ/γ2 chimera can be targeted to either synaptic or extrasynaptic membrane, depending on the α subunit with which it is co-assembled. These experiments suggest that different α subunits directly play a targeting role in guiding GABA$_A$-Rs to synaptic *versus* extrasynaptic sites.

Gephyrin and $GABA_A$-R Targeting—Synaptic $GABA_A$-Rs are thought to be first inserted to extrasynaptic membranes and then laterally diffused into postsynaptic sites, where they are stabilized by the scaffolding protein complex (40, 50, 67, 68). Both knock-out and knockdown of gephyrin expression disrupted the clustering of a major subset of synaptic $GABA_A$-Rs and resulted in decreased GABAergic neurotransmission (28, 40, 50, 69, 70). However, not all $GABA_A$-R clusters are dependent on gephyrin (70, 71). For example, α1-containing receptors in pyramidal neurons are likely stabilized by the dystrophin-glycoprotein complex (27).

The α1–3 subunits, but not the α6 subunit, have been shown to directly bind with gephyrin through their large IL (48, 52, 53). By swapping the IL domain between α2 and α6 subunits, we generated $\alpha2_{\alpha6IL}$ and $\alpha6_{\alpha2IL}$ chimeras to test their targeting role. However, the $\alpha6_{\alpha2IL}\beta3\gamma2$-IPSCs did not show faster kinetics but rather slightly slower than the IPSCs mediated by α6-containing receptors (Fig. 7). Thus, the α2 IL domain alone is not sufficient for the synaptic targeting of $GABA_A$-Rs. In agreement with our finding, a recent study showed that the interaction between $GABA_A$-R α2 subunit and gephyrin is much weaker than that between GlyR β subunit and gephyrin (54).

We hypothesized that the extrasynaptic localization of $\alpha6\beta3\delta$ receptors is due to the lack of interaction with gephyrin. To test this hypothesis, we inserted a high affinity gephyrin-binding site into the IL domain of α6 and δ subunits to force an interaction with gephyrin (38, 72). We showed that $\alpha6\beta3\delta_{GBS}$ IPSCs in HEK cells (with or without gephyrin overexpression) have faster kinetic properties than $\alpha6\beta3\delta$ IPSCs, suggesting that the δ_{GBS} subunit-containing receptors are localized closer to synaptic sites than native δ subunit-containing receptors (Fig. 8). Furthermore, immunostaining in neurons demonstrated that $\alpha6_{GBS}\beta\delta_{GBS}$ receptors form clusters that co-localized with gephyrin and GAD at synapses (Fig. 9). These results suggest that forced interaction with gephyrin is capable of bringing extrasynaptic $\alpha6\beta3\delta$ receptors close to synaptic sites.

To our surprise, gephyrin or collybistin co-expression was not required for the δ_{GBS}-Rs to mediate faster IPSC events (Fig. 8*F*). We hypothesize that endogenous gephyrin in HEK cells is sufficient to interact with δ_{GBS} and target the receptors closer to synaptic membranes. Indeed, we found that a subpopulation of HEK cells expressed a high level of gephyrin, although the rest showed a low level of expression. Interestingly, the HEK cells expressing high levels of gephyrin usually showed compact chromatin structures as revealed by DAPI staining (supplemental Fig. 1). Because gephyrin is a microtubule-binding protein, we suspect that such a high level of expression might indicate a potential role of gephyrin during cell division, which is worthy of future study but is beyond the scope of this work.

Besides $GABA_A$-Rs, recent studies suggest that collybistin and NL2 also interact with gephyrin (1). NL2 has been suggested to interact with gephyrin and collybistin to target $GABA_A$-Rs to perisomatic membranes (73). NL2 overexpression may also change $GABA_A$-R subunit composition as shown in cerebellar granule cells (74). Collybistin can facilitate gephyrin localization to submembrane sites (75) and increase synaptic $GABA_A$-R accumulation (76). Collybistin deficiency results in region-specific loss of gephyrin and a subset of $GABA_A$-Rs, as well as altered synaptic plasticity and increased levels of anxiety (77, 78). Moreover, collybistin and gephyrin may form a complex that is particularly important for interaction with the α2 subunit (79). In this study, we have co-expressed collybistin ($CB3_{SH3+}$ or $CB3_{SH3-}$) with $\alpha6\beta3\delta_{GBS}$ and gephyrin as well as NL2 in HEK cells. Interestingly, GABA current amplitudes were increased by collybistin (data not shown), but the IPSC kinetics were not changed. This may suggest that collybistin contributes to $GABA_A$-R trafficking to the membrane surface but does not affect receptor localization.

Conclusion—Our studies suggest that different $GABA_A$-R subunits encode intrinsic targeting information, and the subcellular localization of a particular subtype of receptor is determined by the integral effect of not only the γ2 and δ subunits but also different α subunits (*e.g.* α2 *versus* α6 subunit). Thus, α subunits not only are required for the assembly of functional receptors but also carry a direct targeting signal for subcellular localization. Our hetero-synapse system provides a unique model for further studying the targeting mechanisms of $GABA_A$ receptors with a variety of subunit partnership.

REFERENCES

1. Luscher, B., Fuchs, T., and Kilpatrick, C. L. (2011) $GABA_A$ receptor trafficking-mediated plasticity of inhibitory synapses. *Neuron* **70,** 385–409
2. Jacob, T. C., Moss, S. J., and Jurd, R. (2008) $GABA_A$ receptor trafficking and its role in the dynamic modulation of neuronal inhibition. *Nat. Rev. Neurosci.* **9,** 331–343
3. Olsen, R. W., and Sieghart, W. (2009) $GABA_A$ receptors. Subtypes provide diversity of function and pharmacology. *Neuropharmacology* **56,** 141–148
4. Sigel, E., Baur, R., Boulineau, N., and Minier, F. (2006) Impact of subunit positioning on GABAA receptor function. *Biochem. Soc. Trans.* **34,** 868–871
5. Farrant, M., and Nusser, Z. (2005) Variations on an inhibitory theme. Phasic and tonic activation of $GABA_A$ receptors. *Nat. Rev. Neurosci.* **6,** 215–229
6. Brickley, S. G., and Mody, I. (2012) Extrasynaptic $GABA_A$ receptors. Their function in the CNS and implications for disease. *Neuron* **73,** 23–34
7. Nusser, Z., Sieghart, W., and Somogyi, P. (1998) Segregation of different $GABA_A$ receptors to synaptic and extrasynaptic membranes of cerebellar granule cells. *J. Neurosci.* **18,** 1693–1703
8. Wei, W., Zhang, N., Peng, Z., Houser, C. R., and Mody, I. (2003) Perisynaptic localization of δ subunit-containing $GABA_A$ receptors and their activation by GABA spillover in the mouse dentate gyrus. *J. Neurosci.* **23,** 10650–10661
9. Glykys, J., Peng, Z., Chandra, D., Homanics, G. E., Houser, C. R., and Mody, I. (2007) A new naturally occurring $GABA_A$ receptor subunit partnership with high sensitivity to ethanol. *Nat. Neurosci.* **10,** 40–48
10. Serwanski, D. R., Miralles, C. P., Christie, S. B., Mehta, A. K., Li, X., and De Blas, A. L. (2006) Synaptic and nonsynaptic localization of $GABA_A$ receptors containing the α5 subunit in the rat brain. *J. Comp. Neurol.* **499,** 458–470
11. Swanwick, C. C., Murthy, N. R., Mtchedlishvili, Z., Sieghart, W., and Kapur, J. (2006) Development of γ-aminobutyric acidergic synapses in cultured hippocampal neurons. *J. Comp. Neurol.* **495,** 497–510
12. Brünig, I., Scotti, E., Sidler, C., and Fritschy, J. M. (2002) Intact sorting, targeting, and clustering of γ-aminobutyric acid A receptor subtypes in hippocampal neurons *in vitro*. *J. Comp. Neurol.* **443,** 43–55
13. Hamann, M., Rossi, D. J., and Attwell, D. (2002) Tonic and spillover inhibition of granule cells control information flow through cerebellar cortex. *Neuron* **33,** 625–633
14. Semyanov, A., Walker, M. C., and Kullmann, D. M. (2003) GABA uptake regulates cortical excitability via cell type-specific tonic inhibition. *Nat. Neurosci.* **6,** 484–490

15. Mody, I. (2005) Aspects of the homeostatic plasticity of $GABA_A$ receptor-mediated inhibition. *J. Physiol.* **562,** 37–46
16. Winsky-Sommerer, R. (2009) Role of $GABA_A$ receptors in the physiology and pharmacology of sleep. *Eur. J. Neurosci.* **29,** 1779–1794
17. Feng, H. J., Kang, J. Q., Song, L., Dibbens, L., Mulley, J., and Macdonald, R. L. (2006) δ subunit susceptibility variants E177A and R220H associated with complex epilepsy alter channel gating and surface expression of $\alpha4\beta2\delta$ $GABA_A$ receptors. *J. Neurosci.* **26,** 1499–1506
18. Damgaard, T., Plath, N., Neill, J. C., and Hansen, S. L. (2011) Extrasynaptic $GABA_A$ receptor activation reverses recognition memory deficits in an animal model of schizophrenia. *Psychopharmacology* **214,** 403–413
19. Vengeliene, V., Bilbao, A., Molander, A., and Spanagel, R. (2008) Neuropharmacology of alcohol addiction. *Br. J. Pharmacol.* **154,** 299–315
20. Martin, L. J., Zurek, A. A., MacDonald, J. F., Roder, J. C., Jackson, M. F., and Orser, B. A. (2010) α5 $GABA_A$ receptor activity sets the threshold for long term potentiation and constrains hippocampus-dependent memory. *J. Neurosci.* **30,** 5269–5282
21. Smith, S. S., Shen, H., Gong, Q. H., and Zhou, X. (2007) Neurosteroid regulation of $GABA_A$ receptors. Focus on the α4 and δ subunits. *Pharmacol. Ther.* **116,** 58–76
22. Maguire, J., and Mody, I. (2008) $GABA_AR$ plasticity during pregnancy. Relevance to postpartum depression. *Neuron* **59,** 207–213
23. Holm, M. M., Nieto-Gonzalez, J. L., Vardya, I., Henningsen, K., Jayatissa, M. N., Wiborg, O., and Jensen, K. (2011) Hippocampal GABAergic dysfunction in a rat chronic mild stress model of depression. *Hippocampus* **21,** 422–433
24. Patrizi, A., Scelfo, B., Viltono, L., Briatore, F., Fukaya, M., Watanabe, M., Strata, P., Varoqueaux, F., Brose, N., Fritschy, J. M., and Sassoè-Pognetto, M. (2008) Synapse formation and clustering of neuroligin-2 in the absence of $GABA_A$ receptors. *Proc. Natl. Acad. Sci. U.S.A.* **105,** 13151–13156
25. Kralic, J. E., Sidler, C., Parpan, F., Homanics, G. E., Morrow, A. L., and Fritschy, J. M. (2006) Compensatory alteration of inhibitory synaptic circuits in cerebellum and thalamus of γ-aminobutyric acid type A receptor α1 subunit knockout mice. *J. Comp. Neurol.* **495,** 408–421
26. Studer, R., von Boehmer, L., Haenggi, T., Schweizer, C., Benke, D., Rudolph, U., and Fritschy, J. M. (2006) Alteration of GABAergic synapses and gephyrin clusters in the thalamic reticular nucleus of $GABA_A$ receptor α3 subunit-null mice. *Eur. J. Neurosci.* **24,** 1307–1315
27. Panzanelli, P., Gunn, B. G., Schlatter, M. C., Benke, D., Tyagarajan, S. K., Scheiffele, P., Belelli, D., Lambert, J. J., Rudolph, U., and Fritschy, J. M. (2011) Distinct mechanisms regulate $GABA_A$ receptor and gephyrin clustering at perisomatic and axo-axonic synapses on CA1 pyramidal cells. *J. Physiol.* **589,** 4959–4980
28. Essrich, C., Lorez, M., Benson, J. A., Fritschy, J. M., and Lüscher, B. (1998) Postsynaptic clustering of major $GABA_A$ receptor subtypes requires the γ2 subunit and gephyrin. *Nat. Neurosci.* **1,** 563–571
29. Li, R. W., Yu, W., Christie, S., Miralles, C. P., Bai, J., Loturco, J. J., and De Blas, A. L. (2005) Disruption of postsynaptic GABA receptor clusters leads to decreased GABAergic innervation of pyramidal neurons. *J. Neurochem.* **95,** 756–770
30. Alldred, M. J., Mulder-Rosi, J., Lingenfelter, S. E., Chen, G., and Lüscher, B. (2005) Distinct γ2 subunit domains mediate clustering and synaptic function of postsynaptic $GABA_A$ receptors and gephyrin. *J. Neurosci.* **25,** 594–603
31. Christie, S. B., Li, R. W., Miralles, C. P., Yang, B. Y., and De Blas, A. L. (2006) Clustered and nonclustered $GABA_A$ receptors in cultured hippocampal neurons. *Mol. Cell. Neurosci.* **31,** 1–14
32. Jiang, M., and Chen, G. (2009) Ca^{2+} regulation of dynamin-independent endocytosis in cortical astrocytes. *J. Neurosci.* **29,** 8063–8074
33. McCarthy, K. D., and de Vellis, J. (1980) Preparation of separate astroglial and oligodendroglial cell cultures from rat cerebral tissue. *J. Cell Biol.* **85,** 890–902
34. Dong, N., Qi, J., and Chen, G. (2007) Molecular reconstitution of functional GABAergic synapses with expression of neuroligin-2 and $GABA_A$ receptors. *Mol. Cell. Neurosci.* **35,** 14–23
35. Jiang, M., and Chen, G. (2006) High Ca^{2+}-phosphate transfection efficiency in low density neuronal cultures. *Nat. Protoc.* **1,** 695–700
36. Bianchi, M. T., Haas, K. F., and Macdonald, R. L. (2002) α1 and α6 subunits specify distinct desensitization, deactivation, and neurosteroid modulation of $GABA_A$ receptors containing the δ subunit. *Neuropharmacology* **43,** 492–502
37. Nagaya, N., and Macdonald, R. L. (2001) Two γ2L subunit domains confer low Zn^{2+} sensitivity to ternary $GABA_A$ receptors. *J. Physiol.* **532,** 17–30
38. Meyer, G., Kirsch, J., Betz, H., and Langosch, D. (1995) Identification of a gephyrin-binding motif on the glycine receptor β subunit. *Neuron* **15,** 563–572
39. Chih, B., Engelman, H., and Scheiffele, P. (2005) Control of excitatory and inhibitory synapse formation by neuroligins. *Science* **307,** 1324–1328
40. Yu, W., Jiang, M., Miralles, C. P., Li, R. W., Chen, G., and de Blas, A. L. (2007) Gephyrin clustering is required for the stability of GABAergic synapses. *Mol. Cell. Neurosci.* **36,** 484–500
41. Kalscheuer, V. M., Musante, L., Fang, C., Hoffmann, K., Fuchs, C., Carta, E., Deas, E., Venkateswarlu, K., Menzel, C., Ullmann, R., Tommerup, N., Dalprà, L., Tzschach, A., Selicorni, A., Lüscher, B., Ropers, H. H., Harvey, K., and Harvey, R. J. (2009) A balanced chromosomal translocation disrupting ARHGEF9 is associated with epilepsy, anxiety, aggression, and mental retardation. *Hum. Mutat.* **30,** 61–68
42. Deng, L., Yao, J., Fang, C., Dong, N., Luscher, B., and Chen, G. (2007) Sequential postsynaptic maturation governs the temporal order of GABAergic and glutamatergic synaptogenesis in rat embryonic cultures. *J. Neurosci.* **27,** 10860–10869
43. Liu, Y., and Dilger, J. P. (1991) Opening rate of acetylcholine receptor channels. *Biophys. J.* **60,** 424–432
44. Andersen, N., Corradi, J., Bartos, M., Sine, S. M., and Bouzat, C. (2011) Functional relationships between agonist-binding sites and coupling regions of homomeric Cys-loop receptors. *J. Neurosci.* **31,** 3662–3669
45. Wohlfarth, K. M., Bianchi, M. T., and Macdonald, R. L. (2002) Enhanced neurosteroid potentiation of ternary $GABA_A$ receptors containing the δ subunit. *J. Neurosci.* **22,** 1541–1549
46. Krogsgaard-Larsen, P., Frølund, B., Liljefors, T., and Ebert, B. (2004) $GABA_A$ agonists and partial agonists. THIP (Gaboxadol) as a nonopioid analgesic and a novel type of hypnotic. *Biochem. Pharmacol.* **68,** 1573–1580
47. Rossi, D. J., and Hamann, M. (1998) Spillover-mediated transmission at inhibitory synapses promoted by high affinity α6 subunit $GABA_A$ receptors and glomerular geometry. *Neuron* **20,** 783–795
48. Tretter, V., Jacob, T. C., Mukherjee, J., Fritschy, J. M., Pangalos, M. N., and Moss, S. J. (2008) The clustering of $GABA_A$ receptor subtypes at inhibitory synapses is facilitated via the direct binding of receptor α2 subunits to gephyrin. *J. Neurosci.* **28,** 1356–1365
49. Craig, A. M., Banker, G., Chang, W., McGrath, M. E., and Serpinskaya, A. S. (1996) Clustering of gephyrin at GABAergic but not glutamatergic synapses in cultured rat hippocampal neurons. *J. Neurosci.* **16,** 3166–3177
50. Jacob, T. C., Bogdanov, Y. D., Magnus, C., Saliba, R. S., Kittler, J. T., Haydon, P. G., and Moss, S. J. (2005) Gephyrin regulates the cell surface dynamics of synaptic $GABA_A$ receptors. *J. Neurosci.* **25,** 10469–10478
51. Sassoè-Pognetto, M., and Fritschy, J. M. (2000) Mini-review. Gephyrin, a major postsynaptic protein of GABAergic synapses. *Eur. J. Neurosci.* **12,** 2205–2210
52. Tretter, V., Kerschner, B., Milenkovic, I., Ramsden, S. L., Ramerstorfer, J., Saiepour, L., Maric, H. M., Moss, S. J., Schindelin, H., Harvey, R. J., Sieghart, W., and Harvey, K. (2011) Molecular basis of the γ-aminobutyric acid A receptor α3 subunit interaction with the clustering protein gephyrin. *J. Biol. Chem.* **286,** 37702–37711
53. Mukherjee, J., Kretschmannova, K., Gouzer, G., Maric, H. M., Ramsden, S., Tretter, V., Harvey, K., Davies, P. A., Triller, A., Schindelin, H., and Moss, S. J. (2011) The residence time of $GABA_ARs$ at inhibitory synapses is determined by direct binding of the receptor α1 subunit to gephyrin. *J. Neurosci.* **31,** 14677–14687
54. Maric, H. M., Mukherjee, J., Tretter, V., Moss, S. J., and Schindelin, H. (2011) Gephyrin-mediated γ-aminobutyric acid type A and glycine receptor clustering relies on a common binding site. *J. Biol. Chem.* **286,** 42105–42114
55. Kim, S., Burette, A., Chung, H. S., Kwon, S. K., Woo, J., Lee, H. W., Kim, K., Kim, H., Weinberg, R. J., and Kim, E. (2006) NGL family PSD-95-interacting adhesion molecules regulate excitatory synapse formation. *Nat. Neu-*

rosci. **9,** 1294–1301
56. Scheiffele, P., Fan, J., Choih, J., Fetter, R., and Serafini, T. (2000) Neuroligin expressed in non-neuronal cells triggers presynaptic development in contacting axons. *Cell* **101,** 657–669
57. Biederer, T., Sara, Y., Mozhayeva, M., Atasoy, D., Liu, X., Kavalali, E. T., and Südhof, T. C. (2002) SynCAM, a synaptic adhesion molecule that drives synapse assembly. *Science* **297,** 1525–1531
58. Linhoff, M. W., Laurén, J., Cassidy, R. M., Dobie, F. A., Takahashi, H., Nygaard, H. B., Airaksinen, M. S., Strittmatter, S. M., and Craig, A. M. (2009) An unbiased expression screen for synaptogenic proteins identifies the LRRTM protein family as synaptic organizers. *Neuron* **61,** 734–749
59. Fu, Z., Washbourne, P., Ortinski, P., and Vicini, S. (2003) Functional excitatory synapses in HEK 293 cells expressing neuroligin and glutamate receptors. *J. Neurophysiol.* **90,** 3950–3957
60. Graf, E. R., Zhang, X., Jin, S. X., Linhoff, M. W., and Craig, A. M. (2004) Neurexins induce differentiation of GABA and glutamate postsynaptic specializations via neuroligins. *Cell* **119,** 1013–1026
61. Sara, Y., Biederer, T., Atasoy, D., Chubykin, A., Mozhayeva, M. G., Südhof, T. C., and Kavalali, E. T. (2005) Selective capability of SynCAM and neuroligin for functional synapse assembly. *J. Neurosci.* **25,** 260–270
62. Sun, C., Cheng, M. C., Qin, R., Liao, D. L., Chen, T. T., Koong, F. J., Chen, G., and Chen, C. H. (2011) Identification and functional characterization of rare mutations of the neuroligin-2 gene (*NLGN2*) associated with schizophrenia. *Hum. Mol. Genet.* **20,** 3042–3051
63. Mody, I., and Pearce, R. A. (2004) Diversity of inhibitory neurotransmission through $GABA_A$ receptors. *Trends Neurosci.* **27,** 569–575
64. Chandra, D., Jia, F., Liang, J., Peng, Z., Suryanarayanan, A., Werner, D. F., Spigelman, I., Houser, C. R., Olsen, R. W., Harrison, N. L., and Homanics, G. E. (2006) $GABA_A$ receptor α 4 subunits mediate extrasynaptic inhibition in thalamus and dentate gyrus and the action of gaboxadol. *Proc. Natl. Acad. Sci. U.S.A.* **103,** 15230–15235
65. Caraiscos, V. B., Elliott, E. M., You-Ten, K. E., Cheng, V. Y., Belelli, D., Newell, J. G., Jackson, M. F., Lambert, J. J., Rosahl, T. W., Wafford, K. A., MacDonald, J. F., and Orser, B. A. (2004) Tonic inhibition in mouse hippocampal CA1 pyramidal neurons is mediated by α5 subunit-containing γ-aminobutyric acid type A receptors. *Proc. Natl. Acad. Sci. U.S.A.* **101,** 3662–3667
66. Brickley, S. G., Revilla, V., Cull-Candy, S. G., Wisden, W., and Farrant, M. (2001) Adaptive regulation of neuronal excitability by a voltage-independent potassium conductance. *Nature* **409,** 88–92
67. Bogdanov, Y., Michels, G., Armstrong-Gold, C., Haydon, P. G., Lindstrom, J., Pangalos, M., and Moss, S. J. (2006) Synaptic $GABA_A$ receptors are directly recruited from their extrasynaptic counterparts. *EMBO J.* **25,** 4381–4389
68. Thomas, P., Mortensen, M., Hosie, A. M., and Smart, T. G. (2005) Dynamic mobility of functional $GABA_A$ receptors at inhibitory synapses. *Nat. Neurosci.* **8,** 889–897
69. Kneussel, M., Brandstätter, J. H., Laube, B., Stahl, S., Müller, U., and Betz, H. (1999) Loss of postsynaptic $GABA_A$ receptor clustering in gephyrin-deficient mice. *J. Neurosci.* **19,** 9289–9297
70. Lévi, S., Logan, S. M., Tovar, K. R., and Craig, A. M. (2004) Gephyrin is critical for glycine receptor clustering but not for the formation of functional GABAergic synapses in hippocampal neurons. *J. Neurosci.* **24,** 207–217
71. Kneussel, M., Brandstätter, J. H., Gasnier, B., Feng, G., Sanes, J. R., and Betz, H. (2001) Gephyrin-independent clustering of postsynaptic $GABA_A$ receptor subtypes. *Mol. Cell. Neurosci.* **17,** 973–982
72. Kins, S., Kuhse, J., Laube, B., Betz, H., and Kirsch, J. (1999) Incorporation of a gephyrin-binding motif targets NMDA receptors to gephyrin-rich domains in HEK 293 cells. *Eur. J. Neurosci.* **11,** 740–744
73. Poulopoulos, A., Aramuni, G., Meyer, G., Soykan, T., Hoon, M., Papadopoulos, T., Zhang, M., Paarmann, I., Fuchs, C., Harvey, K., Jedlicka, P., Schwarzacher, S. W., Betz, H., Harvey, R. J., Brose, N., Zhang, W., and Varoqueaux, F. (2009) Neuroligin 2 drives postsynaptic assembly at perisomatic inhibitory synapses through gephyrin and collybistin. *Neuron* **63,** 628–642
74. Fu, Z., and Vicini, S. (2009) Neuroligin-2 accelerates GABAergic synapse maturation in cerebellar granule cells. *Mol. Cell. Neurosci.* **42,** 45–55
75. Harvey, K., Duguid, I. C., Alldred, M. J., Beatty, S. E., Ward, H., Keep, N. H., Lingenfelter, S. E., Pearce, B. R., Lundgren, J., Owen, M. J., Smart, T. G., Lüscher, B., Rees, M. I., and Harvey, R. J. (2004) The GDP-GTP exchange factor collybistin. An essential determinant of neuronal gephyrin clustering. *J. Neurosci.* **24,** 5816–5826
76. Chiou, T. T., Bonhomme, B., Jin, H., Miralles, C. P., Xiao, H., Fu, Z., Harvey, R. J., Harvey, K., Vicini, S., and De Blas, A. L. (2011) Differential regulation of the postsynaptic clustering of γ-aminobutyric acid type A ($GABA_A$) receptors by collybistin isoforms. *J. Biol. Chem.* **286,** 22456–22468
77. Papadopoulos, T., Korte, M., Eulenburg, V., Kubota, H., Retiounskaia, M., Harvey, R. J., Harvey, K., O'Sullivan, G. A., Laube, B., Hülsmann, S., Geiger, J. R., and Betz, H. (2007) Impaired GABAergic transmission and altered hippocampal synaptic plasticity in collybistin-deficient mice. *EMBO J.* **26,** 3888–3899
78. Jedlicka, P., Papadopoulos, T., Deller, T., Betz, H., and Schwarzacher, S. W. (2009) Increased network excitability and impaired induction of long term potentiation in the dentate gyrus of collybistin-deficient mice *in vivo*. *Mol. Cell. Neurosci.* **41,** 94–100
79. Saiepour, L., Fuchs, C., Patrizi, A., Sassoè-Pognetto, M., Harvey, R. J., and Harvey, K. (2010) Complex role of collybistin and gephyrin in $GABA_A$ receptor clustering. *J. Biol. Chem.* **285,** 29623–29631